Abstract

We present a simple, deterministic energy balance model in this report. The model is designed to represent the atmospheric component of the coupled atmosphere-ocean system. It is a one dimensional, global model with time and space resolutions of one year and 10^{0} of latitude respectively. The model predicts the surface air temperature and estimates the surface freshwater flux diagnostically.

The coupling between the atmospheric model and an ocean model is accomplished by heat and freshwater fluxes at their interface. The heat flux is calculated according to the difference in the surface air temperature and ocean surface temperature, while the freshwater flux is estimated from the latent heat transport in the atmosphere by a diagnostic equation since no explicit hydrologic cycle or water vapour budget is kept in the model. Two parameterizations for the latent heat transport are proposed, which distinguishes the two versions of the model. The assumptions made in the first version are that the total heat transport in the combined system is invariant and that the atmospheric sensible heat transport can be approximated by a diffusion process, whereas in the second version both atmospheric sensible heat and water vapour transport are treated as a diffusion process.

Before proceeding with interactive runs, we study the behaviour of the model in a decoupled mode. Some experiments with initial conditions altered and external forcings changed are carried out to investigate the sensitivity and stability of the model. In particular, the influence of the ice-albedo feedback on model solutions is examined. The results of these experiments may be helpful both in understanding the characteristics of the model and in interpreting results when the model is coupled to an OGCM.

Contents

1 Introduction

The ocean circulation is forced by heat, momentum and freshwater fluxes at the upper boundary—the ocean surface. These fluxes provide a means for the ocean to communicate with the atmosphere above it. On the other hand, the atmosphere is also affected by the ocean state through the interfacial fluxes. For ocean general circulation models (OGCMs) these fluxes must be specified.

There are usually two kinds of options to specify these fluxes for an OGCM. The first one is in a coupled mode; *i.e.* the OGCM will be coupled to an atmospheric general circulation model (AGCM) through the fluxes, like what is happening in the real world. The second one is in a decoupled mode, which means that the OGCM is forced either by some specified fluxes or by fluxes which are determined from the ocean state predicted by the ocean model and a specified atmospheric state. In this case, the atmosphere will not be influenced by the ocean.

Naturally it is ideal to use the coupled mode. However, since a huge amount of computing time is needed both by OGCMs and AGCMs, this kind of coupling is simply too expensive to run. Moreover, as an OGCM is already complicated enough, adding an AGCM may make the interpretation and understanding of a coupled model much more difficult.

In the decoupled mode, climatological data for the atmosphere are used to specify the fluxes. This method has the advantage in that one only needs to deal with the ocean physics. It is simple and practical, thereby making the method the most widely used one in ocean modelling. However, it should be noted that the lack of communication between the atmosphere and the ocean is artificial and may cause problems. It is well established that the thermohaline circulation is sensitive to specified boundary conditions such as heat flux and fresh water flux. This is especially true for the fresh water flux.

A well known example of the problems in the decoupled mode is the "polar halocline catastrophe (PHC)", a term coined by F. Bryan (1986). PHCs are observed in models which use mixed boundary conditions. These models are forced by a specified fresh water flux and a relaxation of the surface temperature to a specified value. The fresh water flux is usually diagnosed from an equilibrium run in which the ocean model is spun up by restoring boundary conditions both on surface temperature and salinity. Most studies (*e.g.* Weaver *et al*, 1993) emphasise the influence of the specified fresh water flux on the collapse of the thermohaline circulation, while a few studies also touch the possible effects of the heat flux. Recently, Zhang *et al.* (1993) investigated the effects of the heat flux associated with the mixed boundary conditions. They point out that the fixed atmospheric temperature is also responsible for the occurrence of a PHC. When the atmospheric temperature is allowed to response to the heat flux in such a way that the heat capacity of the atmosphere is set to be zero, they find that a PHC is less likely to occur. This result demonstrates the necessity of including a simple atmospheric component to improve the boundary conditions for the ocean model.

As the two mentioned modes have their own difficulties, it turns out that we ought to seek an intermediate method to overcome the difficulties. This method, on one side, should allow some communication between the atmosphere and the ocean; and on the other side, the atmospheric component should be so simple that only a small amount of additional computer time is needed. We intend here to develop an atmospheric model which is simple enough to be tractable but still has the essential physics that is relevant to the problem. Energy balance models appear to meet these requirements. Here the only spatial dimension appearing explicitly is latitude, and the only dependent variable is the zonally and vertically averaged temperature. Perhaps they are the simplest class of atmospheric models that might be considered for ocean modelling.

To start with, we develop a simple one dimensional EBM which has the ability to predict surface air temperature and to diagnose the fresh water flux. It is hoped that the coupling of this EBM to an OGCM will help to establish an intermediate way to study long term change in coupled ocean-atmosphere system.

The outline of the report is as follows: We shall first formulate the atmospheric model and the coupling between the atmospheric model and ocean model in section 2. There, a detailed description of all parameterizations employed to represent relevant processes is also given. Then in section 3 two versions of the atmospheric model, in which only the heat transport parameterizations are different, are critically tested. In order to identify the model stability and sensitivity, some experiments with regard to different perturbations and the parameterization schemes used by the model are carried out. At last, a summary can be found in section 4.

2 Formulation of the coupled system

2.1 Governing equation of the atmospheric model

We shall start with the thermodynamic equation applied to the atmosphere in isobaric co-ordinates:

$$\frac{d}{dt}(C_pT) = C_p\frac{\partial T}{\partial t} + \mathbf{V}\cdot\nabla C_pT + \omega\frac{\partial C_pT}{\partial p} = h + \frac{RT}{p}\omega \tag{1}$$

where C_p is the specific heat at constant pressure, T atmospheric temperature, t time, $\mathbf{V}$ and ∇ horizontal vector of wind and gradient operator, p pressure, ω vertical wind, and h diabatic heating rate of the atmosphere.

The mass continuity equation may be written as

$$\nabla\cdot\mathbf{V} + \frac{\partial\omega}{\partial p} = 0. \tag{2}$$

Inserting (2) into (1) we have

$$C_p\frac{\partial T}{\partial t} = h - \nabla\cdot(C_pT\mathbf{V}) - \frac{\partial C_pT\omega}{\partial p} + \frac{RT}{p}\omega. \tag{3}$$

Integrating (3) from bottom ($p = p_0$) to top ($p = 0$) of the atmosphere, and assuming $\omega = 0$ at the top and the bottom, we obtain

$$\frac{1}{g}\int_0^{p_0} C_p\frac{\partial T}{\partial t}dp = \frac{1}{g}\int_0^{p_0} hdp - \frac{1}{g}\int_0^{p_0}\nabla\cdot(C_pT\mathbf{V})dp + \frac{1}{g}\int_0^{p_0}\frac{RT}{p}\omega dp. \tag{4}$$

Equation (4) states that the vertically integrated temperature in an air column extending from the bottom to the top of the atmosphere will be influenced by diabatic and adiabatic processes occurring in the column and at the boundary of it.

For an one dimensional model which has only latitudinal resolution, zonally averaging must be made. Also, as the time-scale of our interest is at least several years, time-average of one year is performed. If an overbar and a bracket are used to denote the zonal mean and time mean operators respectively, the governing equation of the atmosphere can be written as

$$\frac{1}{g}\int_0^{p_0}\left[C_p\frac{\partial\bar{T}}{\partial t}\right]dp = \frac{1}{g}\int_0^{p_0}\left[\bar{h}\right]dp - \frac{1}{g}\int_0^{p_0}\nabla\cdot[\overline{C_pT\mathbf{V}}]dp + \frac{1}{g}\int_0^{p_0}\left[\overline{\frac{RT}{p}\omega}\right]dp. \qquad (5)$$

The adiabatic processes are associated with the advection of temperature and temperature changes due to expansion or contraction of an air parcel. The latter is represented by the last term on the right-hand side of (5). The globally averaged value of this term is equal to the dissipation of kinetic energy which is about 5 Wm^{-2} (White and Saltzman, 1956). As this is relatively small compared with the other two terms on the right-hand side of (5), and it is difficult to make an estimate of it, the term will be neglected from now on. Equation (5) then reduces to

$$\frac{1}{g}\int_0^{p_0}\left[C_p\frac{\partial\bar{T}}{\partial t}\right]dp = \frac{1}{g}\int_0^{p_0}\left[\bar{h}\right]dp - \frac{1}{g}\int_0^{p_0}\nabla\cdot[\overline{C_pT\mathbf{V}}]dp \qquad (6)$$

Diabatic processes include radiative heating or cooling , heating due to latent heat release and frictional dissipation and turbulent heat exchange. If the friction is neglected, the first term on the right-hand side of (6) may be expressed as

$$\frac{1}{g}\int_0^{p_0}[\bar{h}]dp = [\bar{R}_t] - [\bar{R}_b] + L[\bar{P}] + [\overline{SH}] \qquad (7)$$

where R_t and R_b are downward net radiative fluxes at the top ($p = 0$) and the bottom ($p = p_0$) of the atmosphere, P is the latent heat release measured by precipitation at the ground, and SH is the sensible heat released from the ground to the atmosphere.

The second term on the right-hand side of (6) is the vertically integrated divergence of sensible heat flux in the atmosphere. This term will be written as

$$div[\bar{F_s}] = \frac{1}{g}\int_0^{p_0} \nabla \cdot [\overline{C_p T \mathbf{V}}] dp \tag{8}$$

where $[\bar{F_s}]$ is the vertically integrated sensible heat flux across a latitude in the atmosphere.

Note that the term $div[\bar{F_S}]$ results from the transport of internal plus potential energy in the p system (see *e.g.* Holton, 1979). But for convenience, it is simply called sensible heat divergence hereafter.

Analogous to the derivation of equation (3), the conservation for water vapour in the atmosphere may be written as

$$\frac{\partial q}{\partial t} + \nabla \cdot (q\mathbf{V}) + \frac{\partial q\omega}{\partial p} = s \tag{9}$$

where q is mixing ratio of atmospheric water vapour, and s describes the sources and sinks of the water vapour.

Performing the vertical integration and temporal plus zonal averaging on (9), it follows that

$$\frac{1}{g}\int_0^{p_0} \frac{\partial[\bar{q}]}{\partial t} dp + \frac{1}{g}\int_0^{p_0} \nabla \cdot [\overline{q\mathbf{V}}] dp = L\left([\bar{E}] - [\bar{P}]\right) \tag{10}$$

where the difference between the evaporation (E) and the precipitation (P) repsents the net supply of the water vapour. Since the interval of the time averaging is one year, the first term on the left-hand side of (10) may be ignored, which leads to

$$div[\bar{F_l}] = L\left([\bar{E}] - [\bar{P}]\right) \tag{11}$$

where $[\bar{F}_l]$ is the vertically integrated latent heat flux in the atmosphere and

$$div[\bar{F}_l] = \frac{1}{g}\int_0^{p_0} \nabla \cdot [\overline{q\mathbf{V}}]dp \tag{12}$$

is the vertically integrated divergence of latent heat flux in the atmosphere. Thus the fresh water flux at the ground ($[\bar{P}] - [\bar{E}]$) is associated with the latent heat transport in the atmosphere.

For the sake of simplicity, all overbars and brackets will subsequently be dropped. Substituting (11) into (7), we arrive at the governing equation for the atmospheric model:

$$\frac{1}{g}\int_0^{p_0} C_p \frac{\partial T}{\partial t} dp = -div\, F_s - div\, F_l + R_t - F_{oa} \tag{13}$$

where F_{oa} is the sum of all downward heat flues at the ground,

$$F_{oa} = R_b - SH - LE. \tag{14}$$

Note that the annual average of F_{oa} vanishes over land surfaces, so it is the heat exchange between the atmosphere and ocean that accounts for F_{oa}. If a subscript o denotes the zonal mean downward fluxes at the ocean surface, and f_o is the fraction of area covered by ocean in a latitude zone, we have

$$F_{oa} = f_o(R_{so} - SH_o - LE_o). \tag{15}$$

2.2 Coupling between the atmosphere and ocean

In the previous section we have derived the governing equation for the atmosphere from the first law of thermodynamics. To illustrate the coupling between the atmosphere and ocean represented by the derived atmospheric model and an OGCM, we need a simplified equation to represent the ocean model. The vertically integrated energy balance equation for the ocean may be written as

$$ST_o = F_{oa} - divF_o \tag{16}$$

where ST_o is the vertically integrated heat storage in the ocean, and $divF_o$ is the vertically integrated sensible heat divergence in the ocean.

Equation (16) gives rise to the first coupling between the model atmosphere and model ocean through heat fluxes at their interface. Following Haney (1971), the sum of all interfacial heat fluxes can be parameterized in terms of the difference in surface air temperature and ocean surface temperature (SST),

$$R_{so} - SH_o - LE_o = \frac{1}{C_{po}\rho_o D\tau}(T_0 - SST) \tag{17}$$

where C_{po} is the specific heat of sea water, D the depth of the top layer of the ocean model, and τ is the time constant which is chosen to be 30 days. Note the surface atmospheric temperature instead of an apparent temperature defined by Haney is used in estimating the total heat flux. As is shown by Haney, the apparent temperature is almost identical with the surface air temperature except in the tropics, where the apparent temperature is a little higher than the air temperature. However, it is generally believed that the difference between the two temperatures in the tropics has minor influence on the model simulations.

The second coupling of the two components is through the freshwater flux at the ocean surface. Since longitudinal variations are not taken into account in this study, we assume that this flux is evenly distributed over land and ocean surface, which means the flux is zonally invariant. This flux is approximately related to the virtual salt flux Q_s^* at the ocean's surface by

$$P - E = \frac{L\rho_*}{S_*}Q_s^* \tag{18}$$

where ρ_* and S_* are reference density and salinity of the sea water.

The coupling by the momentum flux through the interface is ignored in this study. It is believed that the coupling is important for large scale thermohaline circulation. The fixed wind stress distribution is prescribed for the ocean model.

In order to be able to solve the governing equation of the atmospheric model, we need to parameterize the processes in the atmosphere and at the interface. These parameterizations will be described in the following subsection.

2.3 Parameterizations

2.3.1 Relationship between vertically integrated temperature and surface air temperature

As is shown in the preceding section, we can compute the vertically integrated temperature as long as we know the vertically integrated diabatic heating and advection. However, as we are interested in the coupling between the atmosphere and ocean, the air temperature at the sea level rather than the vertically integrated temperature would be directly relevant. Therefore, we need to establish a relationship between the vertically integrated temperature and the surface air temperature.

The vertical structure of the zonally averaged atmospheric temperature has been studied by Rennick (1977). She analyses the data from Oort and Rasmusson (1971) and Taljaard *et al.* (1969), and concludes that the local vertical gradients of the zonally averaged potential temperature at different levels are essentially constant, although they vary with latitude. Based on this finding, temperature at any given altitude in the troposphere may be expressed as a function of surface air temperature and the vertical gradient of the atmospheric potential temperature at a particular latitude. If g_0 is used to denote the vertical gradient, the functional form linking surface air temperature and air temperature in the troposphere will be

$$T(p) = \left(\frac{p}{p_0}\right)^k T_0 - \left(\frac{p}{p_0}\right)^k g_0 \left(p_0 - p\right) \tag{19}$$

where the subscript 0 refers to the sea level which is taken to be 1000 mb, and $k = R/C_p$ (R is the gas constant for dry air).

It is assumed by Rennick that the temperature above the tropopause remains the same as the temperature at the level of the tropopause ($p = p_t$). Expressed in mb, p_t is parameterized by Rennick as

$$p_t = 1581.35 - 4.64 T_0. \tag{20}$$

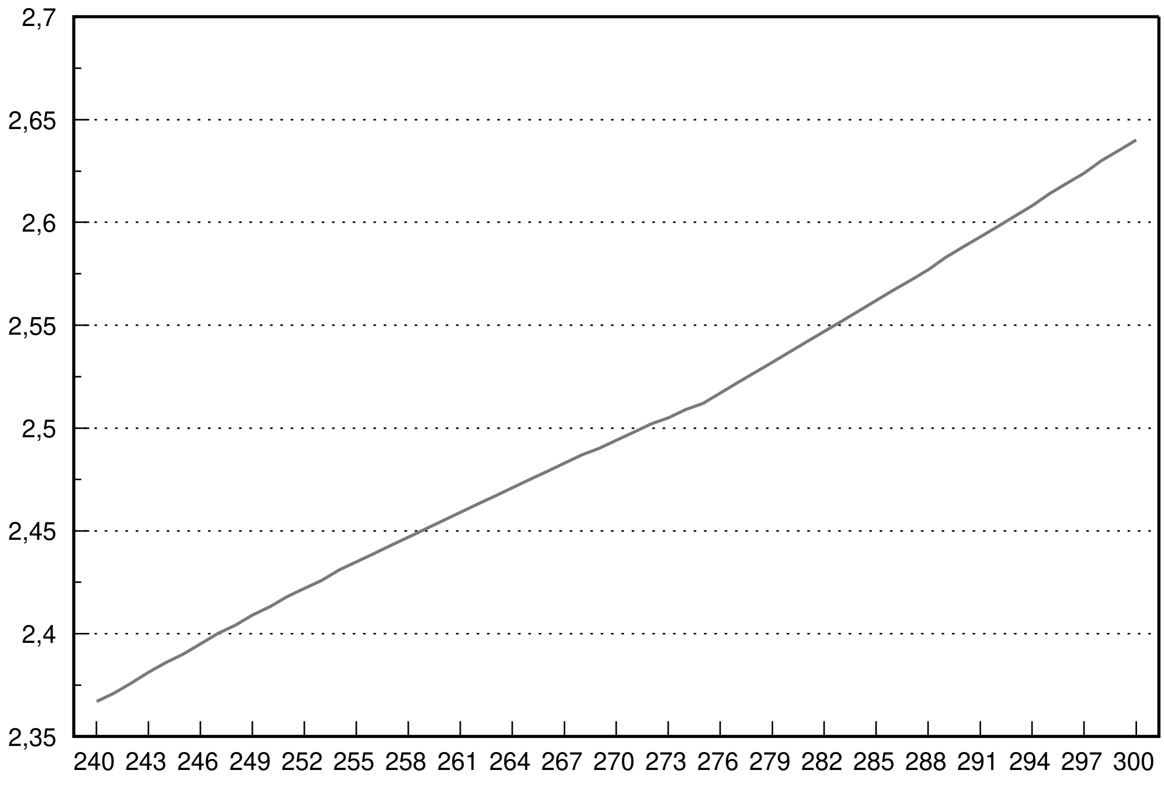

Figure 1: The relationship between the vertically integrated temperature and the surface temperature. The horizontal coordinate represents the surface air temperature T_0 in K, whereas the vertical coordinate shows the vertically integrated temperature $\frac{1}{g}\int_0^{p_0} T dp$ in $10^6\ K\ kgm^{-2}$

In her paper g_0 is parameterized in terms of the surface temperature and the moist adiabatic lapse rate at the surface (g_s) which again can be calculated by the surface air temperature,

$$g_0 = (r_0 + r_1 T_0 + r_2 T_0^2 + r_3 T_0^3)\, g_s \tag{21}$$

where r_i are empirical constants, $r_i = (2.8 \times 10^3, -2.9 \times 10^1, 1.0 \times 10^{-1}, -1.2 \times 10^{-4})$.

From equations (19) through (21) we can calculate the vertically integrated temperature as a function of the surface air temperature. The result is shown in Figure 1.

It is seen from the Figure that there appears to be a nearly linear relation between the two temperatures. However, closer inspection of the curve reveals that the curve can be much better represented by two straight lines with different slopes instead of one straight line. The two lines join together at about 275 K. For the present climate, this temperature is observed at about 50 ${}^0{}^S_N$. Thus it is concluded that two distinct linear relationships exist for low-middle latitudes and high latitudes. These relationships can be represented by the following equations:

$$\frac{1}{g}\int_0^{p_0} \frac{\partial T}{\partial t} dp = \beta\, \frac{\partial T_0}{\partial t}\,; \tag{22}$$

and

$$\beta = \begin{cases} 5708\ kg\, m^{-2} & \text{for } T_0 \geq 275\ K \\ 3966\ kg\, m^{-2} & \text{for } T_0 < 275\ K\ . \end{cases} \tag{23}$$

One-layer EBMs have to deal with the problem of relating the surface air temperature to the vertically averaged temperature. This result is interesting for such a simple EBM because it shows that the surface air temperature can be related to the vertically averaged temperature through two constants globally. The usual assumption made with one-layer EBM so far is that the two temperatures can be related to each other with a single constant globally. Unfortunately, this assumption comes neither from theoretical reasoning nor from empirical estimation. The single constant used by many EBMs are therefore more or less arbitrary.

This calculation may provide an empirical means to estimate the single constant used by many time dependent EBMs. As indicated by the result, should just one constant be used for the global atmosphere, the best choice would be 5300 $kg\,m^{-2}$. Actually, from the unit of β we can see that $\beta\,C_p$ can be interpreted as thermal inertia ($Jm^{-2}K^{-1}$) of a column of air.

The constant $\beta\,C_p$ is written as $\rho_a H_a$ in some EBMs. Here ρ_a and H_a are surface atmospheric density and an effective atmosphere height, respectively. For example, Stocker *et al.* (1992) specify $\rho_a = 1.225\ kg\,m^{-3}$ and $H_a = 8320\ m$. According to our result, H_a should be equal to 4327 m if the same density is used. Thus, the two different constants found in this study simply represent the two different heat capacities of the air column in two different latitude-zones as it is 'felt' by the surface air temperature. As the density does not change so much, this implies that the difference exists mainly in the effective height of the atmosphere.

It is also worth noting that the heat capacity of the air column determines the time scale of the atmospheric thermal response to forcings in the general case while it is a dummy variable in the equilibrium state. This can explain the astonishing success of simple EBMs in simulating equilibrium climate states. It is desirable, however, that the constants be determined on a sound basis when we are to study the interaction between the atmosphere and ocean.

2.3.2 Net radiative flux at the top of the atmosphere

The net radiative flux at the top of the atmosphere (R_t) can be expressed by

$$R_t = Q(1 - \alpha_p) - I \tag{24}$$

where Q is the extraterrestrial insulation, α_p is the planetary albedo, and I is the outgoing infrared radiation.

The incoming solar radiation is calculated by

$$Q = S_0 \, \mu \tag{25}$$

where S_0 is the solar constant, and μ is an annual averaged cosine zenith angle multiplied by fractional daylight time, which is calculated by the $5th$ order polynomial given by Roads and Vallis (1984),

$$\mu = \frac{1}{2} \sum_{i=0}^{5} a_i x^i \tag{26}$$

where $x = 2 \mid \phi \mid / \pi$, ϕ is the latitude in radius, and a_i=(0.61632, -0.11209, 0.110536, -2.1097, 2.28883, -0.54153).

Following Sellers (1969), α_p is made a function of the surface air temperature and latitude,

$$\alpha_p = \begin{cases} b(\phi) + fT_0 & \text{for } T_0 < 283\ K \\ \alpha_p^o & \text{for } T_0 \geq 283\ K \end{cases} \tag{27}$$

where α_p^o is the observed planetary albedo for the present climate, $f = \partial \alpha_p / \partial T_0$ is the so called ice-albedo feedback factor which is a measure of the strength of the ice-albedo feedbackand, and b is a latitude-dependent constant. As we believe that this parameter is important for the model sensitivity, we will vary f to study effect of this parameter. Once f is chosen, b is calculated by matching the estimated α_p to α_p^o using the observed temperature at a latitude zone. Through the introduction of f the parameterization incorporates in a simple way the adjustable positive feedback due to high albedo of snow and sea ice.

The outgoing long wave radiation is estimated using the parameterization proposed by Budyko (1969),

$$I = A + BT_0 \tag{28}$$

where A and B are empirical constants.

2.3.3 Meridional heat transport

In the coupled atmosphere-ocean system, heat transport is accomplished by three types of heat fluxes in the media; namely, the sensible and latent heat transport in the atmosphere and the sensible heat transport in the ocean. While the oceanic heat transport is explicitly computed by the ocean model, the atmospheric heat fluxes must be determined by the atmospheric model. Both the oceanic and atmospheric heat transport are important because they interact with each other through the heat flux at their interface.

We understand that, from the derivation of the temperature and freshwater equations, the surface temperature is affected by the sensible and the latent heat transport in the atmosphere, while the freshwater flux is only determined by the latent heat transport. In the following two subsections we describe two different parameterization schemes for the atmospheric heat transport. It is these two schemes that leads to two versions of the model.

Version one Manabe and Bryan (1985) have studied the heat transport in the atmosphere and the ocean under different CO_2 forcings using a coupled AGCM and OGCM. They find that the total heat transport by the combined system is relatively insensitive to different atmospheric CO_2 concentrations ranging from 150 ppm to 2400 ppm. This is particularly true for the range of 300 ppm to 2400 ppm. This is due to the negligible change in intensity of the thermohaline circulation in the model ocean and the compensation in changes of sensible and latent heat transport in the atmosphere.

Based on this finding, the total heat transport will be kept at its present climatological value. In this way, the atmospheric heat transport $(F_l + F_s)$ can be determined by subtracting the oceanic transport F_o from the specified total transport F.

In order to estimate the precipitation minus evaporation rate, however, we need to know F_l. As F_s is more readily related to the meridional gradient of the surface air temperature, we parameterize it as

$$F_s = -K_s \frac{\partial T_0}{\partial y} \tag{29}$$

where K_s is diffusion coefficient for the atmospheric sensible heat. K_s will be determined by fitting the related climatological data and be kept constant. Once F_s is known, it is straightforward to calculate F_l. Finally the evaporation minus precipitation rate will be diagnostically computed by equation (11).

Obviously the determination of F_l is essential to the estimation of the freshwater flux. For that reason we would like to try the second parameterization for the heat transport in order to test the influence of the transport schemes on the freshwater flux. By studying the performances of the schemes it may be possible to judge which one is more appropriate for the formulation of the coupled system.

Version two The second parameterization is different from the first one in that the total heat transport is no longer invariant. Thus we need to parameterize the sensible and latent heat transport in the atmosphere separately. However, the two fluxes are not totally independent. Actually, they are all related to the meridional gradient of the surface air temperature.

If we assume that the flux of moisture, like that of temperature, can be approximated by a diffusion process, the latent heat flux may be written as

$$F_l = -K_l \frac{L}{C_p} \frac{\partial q}{\partial y} \tag{30}$$

where K_l is the diffusion coefficient for water vapour in the atmosphere.

It is well known that q can be related to temperature through the relative humidity RH by the following equation:

$$q = \frac{e_s(T_0)}{p_0} RH \tag{31}$$

where e_s is the saturation water vapour pressure, which is a function of temperature T_0 only,

$$e_s = 0.622 \times 10^{C_1 - C_2/T_0} \tag{32}$$

where C_1 and C_2 are empirical constants:

$$C_1 = \begin{cases} 9.4051 & \text{for } T_0 \geq 273\ K \\ 10.553 & \text{for } T_0 < 273\ K\ , \end{cases} \tag{33}$$

and

$$C_2 = \begin{cases} 2354 & \text{for } T_0 \geq 273\ K \\ 2667 & \text{for } T_0 < 273\ K\ . \end{cases} \tag{34}$$

If we make a further assumption that the relative humidity remains constant, which is a quite often used assumption in climate modelling, we can rewrite the equation (30) as

$$F_l = -K_l \frac{L}{C_p} RH \frac{\partial q_s}{\partial T_0} \frac{\partial T_0}{\partial y} \tag{35}$$

where q_s is the saturation mixing ratio of the water vapour.

2.4 Tuning Procedure

Before we can work with the model, all empirical constants involved in the parameterizations discussed in the previous subsection have to be determined. For this purpose we need a set of *consistent* data which describes a known climate state. By consistent we mean that the data should match the model physics and therefore satisfy the governing equations of the combined system. Apparently, climatological data is a good candidate since we need just to deal with the equilibrium state.

In calibrating the model parameterizations, the satellite data of outgoing radiation, net radiation and planetary albedo from Stephens *et al.* (1981), surface air temperature from Oort (1983), and latent heat transport from Sellers (1969) will be used. It should be kept in mind that these data are not averaged over the same period of time and there may be errors in them. Furthermore, the length of observational records may not be long enough to be representative for an equilibrium state of the atmosphere-ocean system. Therefore, these data will be checked against the governing equations and will be manipulated, if necessary, so that they will obey the model physics.

2.4.1 Total heat transport

Adding (16) into (13) and assuming the coupled ocean-atmosphere is in equilibrium, we have

$$divF = R_t \tag{36}$$

where

$$F = F_l + F_s + F_o \tag{37}$$

is the total northward heat transport in the coupled atmosphere-ocean system.

By integrating (36) with the observed radiation balance, we should be able to get F.

If we start integration from one pole where the heat transport vanishes, then we do not arrive at zero heat transport at the other pole. In other words, the globally integrated heat divergence implied by the radiation data from Stephens *et al.* is not zero. This may be due to errors in the data and the relative short observation period.

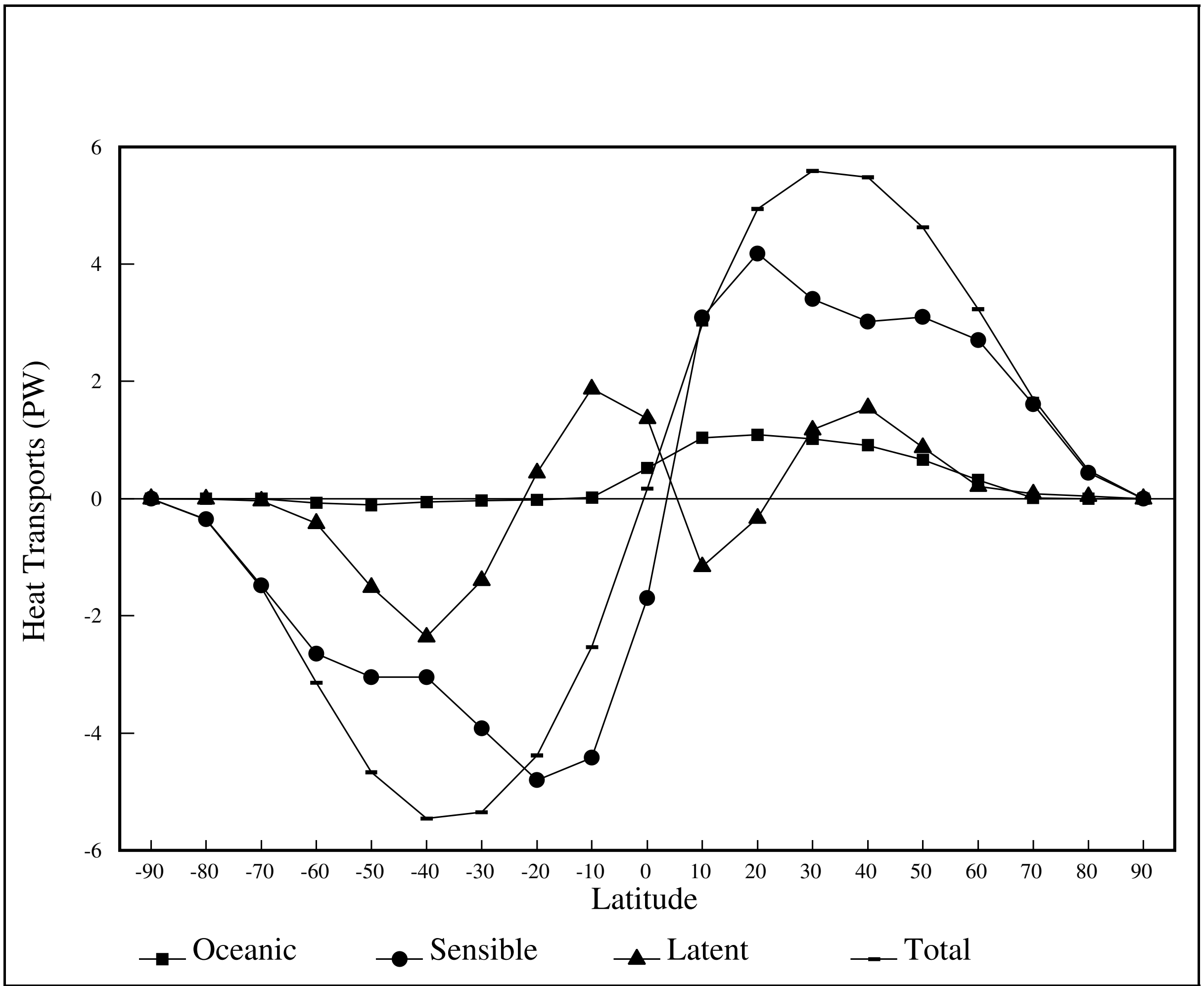

Figure 2: Components of the heat transport in the combined system: The total transport is estimated using the net radiation flux data from Stephens *et al.*, the latent transport is from Sellers, the oceanic transport is from an equilibrium run of our global ocean model, and the sensible transport is calculated as a residual the total transport from all other components.

The simplest way to overcome this difficulty is to subtract from the original radiation data at each latitude zone their global mean and use this 'corrected' value of R_t in the integration. The global mean value of R_t for the data used is 9 Wm^{-2}. The total heat transport in the combined ocean-atmosphere system calculated in this way is displayed in Figure 2. The total transport compares favourably with the estimate by Carissimo *et* *al.* (1985) and others (not shown).

2.4.2 Outgoing longwave radiation

The fact that the globally integrated total transport inferred from the satellite data is not zero makes it impossible to use the data as a proper representative of an equilibrium state. Besides, the incoming solar radiation is calculated by (25) in the model which may not be necessarily identical to that implied by the satellite data though the difference is quite small. Thus the original data has been modified to meet the requirements of equation (36). The correction made is associated with the net radiation. Thus, we may transfer this correction to either ougtgoing radiation or planetary albedo, or both. We choose to correct the outgoing radiation data simply because of its relatively great magnitude. This correction of about 9 Wm^{-2} usually amounts to 5 per cent of its normal value.

The modified outgoing radiation and the temperature data are used to estimate A and B in (28). A linear correlation is applied and the best fit of the data shows that $A = 213.35\ Wm^{-2}$ and $B = 2.22\ Wm^{-2}K^{-1}$. The correlation coefficient is found to be 0.98. In all cases the variance of the outgoing radiation explained by the relation along with the estimated coefficients is about 95 per cent.

2.4.3 Diffusion coefficients

For the two versions of the model, we need to determine the eddy coefficient for sensible heat. It is estimated by the sensible flux and the temperature data at each latitude belt based on (29).

The partitioning of the total heat transport among its components differs considerably using different data sources and estimation methods, while the total transport appears to be almost the same. This raises the question of how the decomposition of the the atmospheric transport into latent and sensible transports should be done in our model?

Of course we need first to compute the oceanic transport before we can estimate the atmospheric transport and answer the question raised. For that purpose we use an OGCM which will be coupled to the EBM. The OGCM is the GFDL code known as mom.

(Pacanowski *et al.*, 1991). The ocean model extends from 66 ^0S to 80 ^0N in latitude and from 60 ^0W to 14 ^0E in longitude. Thus it has only a single basin with a width of 74 ^{0} of longitude. The horizontal resolution of the model is $2^0 \times 2^0$, while in the vertical it has 15 levels. The depth of the ocean is 5700 m everywhere.

For the sake of greatest possible consistency, the ocean model is forced by the atmospheric temperature from Oort and a prescribed surface salinity through Newtonian damping terms acting at the uppermost level. The ocean model is integrated until equilibrium is reached. Then the longitudinally averaged heat transport is computed. The result is displayed in Figure 2. This oceanic heat transport is used in estimating the diffusion coefficients and in all experiments to be described in the next section.

Now we turn to the question of how to divide the atmospheric transport into latent and sensible transport. We found if we use the sensible heat flux from Sellers, we will get a much higher latent heat transport since the oceanic transport from Sellers is much larger than that of our ocean model.

Considering the importance of the latent heat transport for the freshwater flux determination, we chose to use the latent heat flux of Sellers plus the estimated oceanic transport and the specified total transport to calculate the sensible heat flux as a residual. Then we will use this adjusted flux to compute the diffusion coefficient. In other words, the sensible heat flux is tuned so that the latent heat flux is the same as that from Sellers given the total transport and the oceanic transport of the ocean model. The adjusted sensible heat flux, along with the latent and total heat transport used, is also displayed in Figure 2. We see that the maximum value of the sensible heat flux is about $\pm 4.5 PW$ ($1\,PW = 10^{15}\,W$) which is somewhat (about 1.5 PW) greater than estimated by radiosonde observations. However, it is found that AGCM simulations usually have significant greater value of atmospheric transport than indicated from the radiosonde observations, which is argued by Covey (1988) to be more closer to the truth. It should also be pointed out that since the climatology of F_s is estimated as a residual, its value may include errors in all involved terms.

The latitudinal profile of the diffusion coefficient for the sensible heat calculated in this way is shown in Figure 3. Note that $K_s/\beta C_p$ rather than K_s is displayed. It is seen that the coefficient varies from $10^5\ m^2s^{-1}$ to $10^7\ m^2s^{-1}$. The diffusion coefficient peeks at equator, which can be explained by the very small meridional temperature gradient there. The almost evenly distributed diffusion coefficient in middle and high latitudes may be an indication that the transport processes there may be well approximated by a diffusion process.

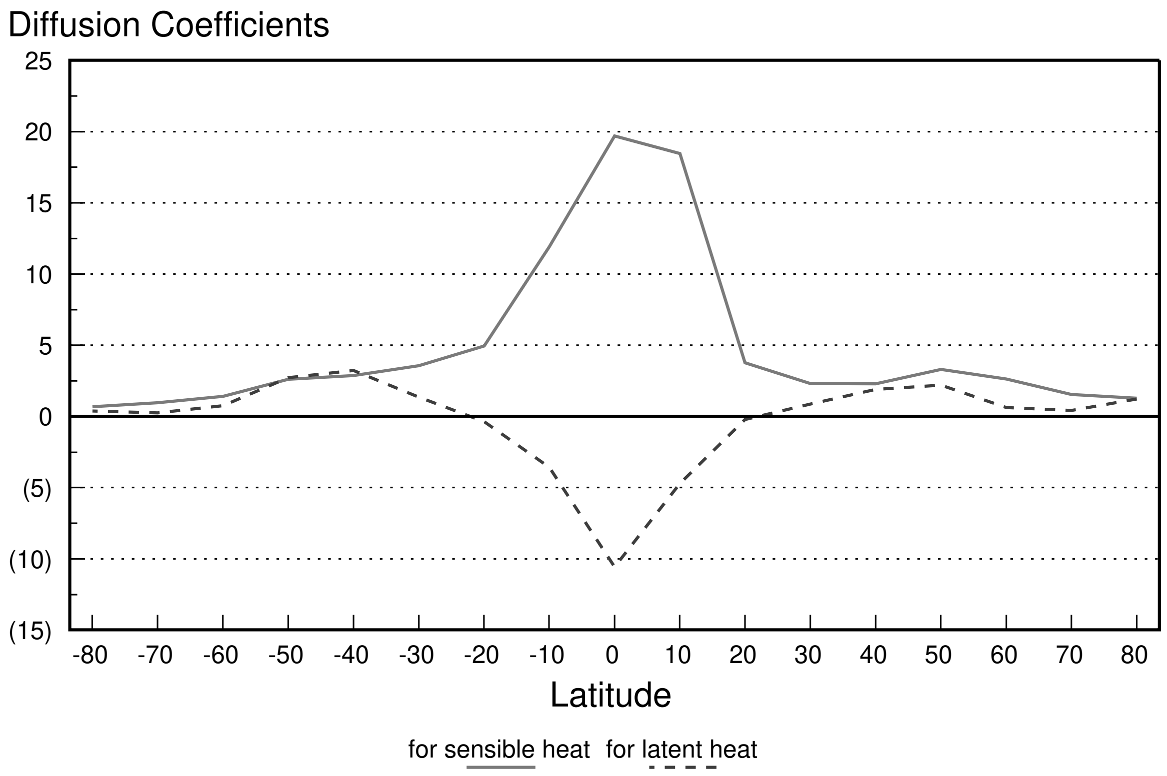

Figure 3: Latitudinal distribution of the diffusion coefficients for the sensible ($K_s/\beta C_p$) and the latent ($K_l/\beta C_p$) heat transports in the atmosphere. Note that the later one is used only in the second version of the atmospheric model that calculates the latent heat transport explicitly. The unit of the diffusion coefficients is $10^6\, m^2 s^{-1}$.

For the second version, the diffusion coefficient for the latent heat also needs to be determined. Using the climatology of the temperature and the latent heat flux, the diffusion coefficient for water vapour is calculated and shown in Figure 3. In the calculation the relative humidity RH is taken as 0.8 everywhere. Also, $K_l/\beta C_p$ rather than K_l is displayed. The diffusion coefficient for the latent heat transport has the same order of magnitude as that for the sensible heat transport in the extratropics. Negative values appear in the tropics, as is also found by Ghil (1976) and Harvey (1988).

The negative diffusion coefficient for the latent heat implies that the diffusion parameterization does not represent the transport process in the tropics well. Indeed, the dominant dynamic processes there are advective rather than diffusive. As has been shown by Oort and Rusmusson (1970), the dominant mechanism of transport in the tropics is the mean meridional circulation, known as the Hadley circulation. As the water vapour is concentrated in the lower part of the troposphere, where the equatorward motion dominates, the vertically integrated water vapor transport is counter gradient, rather than down gradient. This leads to the negative diffusion ciefficients for the latent heat transport.

However, as long as we use the coefficient in the diagnostic equation (35), we do not expect the negative values to cause troubles. Also, in the prognostic equation in version 2, it is the sum of the latent and sensible transport, not the latent transport alone, that enters the differential equation. So the atmospherc heat transport F_a can be written as follows:

$$F_a = F_l + F_s = -K_a \frac{\partial T_0}{\partial y} \tag{38}$$

where

$$K_a = K_s + K_l \frac{L}{C_p} RH \frac{\partial q_s}{\partial T_0} \tag{39}$$

is an effective diffusion coefficient for the total atmospheric transport. We found that in all experiments K_a remains positive, implying that the atmospherric transport is down gradient. Therefore, it is concluded that numerically the negative K_l will not be troublesome. Note that K_a is temperature dependent.

2.4.4 Consistent factor

At this stage, it is found that when the model is run using the parameterizations calibrated, we can not yet get the right temperature distribution. The difference between the simulated and the observed temperature can be as high as 5 K. This is not surprising since the model temperature is strongly determined by the outgoing radiation. As there is still 5 per cent of the radiation variation not explained by the linear parameterization (28), the predicted temperature will be affected by the error in that part of the radiation.

In order to be able to capture this part of the radiation, we added clouds as an additional variable in the parameterization of the outgoing radiation. However, adding clouds has only a negligible effect on the performance of the model though it does have some positive influence. We understand that the radiation is also affected by the stratification of the atmosphere, surface temperature and other factors. Thus it is understandable that the radiation can not be perfectly predicted by the surface air temperature alone.

Considering that clouds and other parameters which influence the outgoing radiation are not variables of the model, including these factors does not add any freedom to the model. We could, however, add a tuneable parameter to the parameterization. The parameter should take into account the effect of all unknown factors. So we have

$$I = CF(A + BT_0) \tag{40}$$

where CF is the tuneable parameter and is called 'consistent factor' by Schneider (1977). CF is estimated from the parameterization for the outgoing radiation and the temperature from Oort. It is found that CF varies between 0.94-1.07, which is considered to be relatively small. In the model we will use (40) instead of (28) to calculate the outgoing radiation.

For the reader's convenience, the adjusted data used to calibrate the parameterizations are listed in Table 1. The components of heat transport and the estimated diffusion coefficients used are shown in Table 2.

Table 1: Calibrating parameters used: T_0 from Oort (1983), R_t is estimated by subtracting its global mean out from the data of Stephens *et al.* (1981) (see text), Q is calculated by (25) with $S_0 = 1376\ Wm^{-2}$, α_p is from Stephens *et al.* (1981) also, I is calculated from (24) with R_t, Q, and α_p in the Table, and CF is computed from (28) with T_0 and the corrected I in the Table.

Latitude	T_0,^0C	R_t,Wm^{-2}	Q,Wm^{-2}	I,Wm^{-2}	α_p	CF
$85^0\ S$	-29.3	-92	169	143	0.70	0.96
$75^0\ S$	-21.2	-101	182	167	0.64	1.00
$65^0\ S$	-8.8	-86	216	192	0.51	0.99
$55^0\ S$	1.4	-60	262	212	0.42	0.98
$45^0\ S$	8.7	-25	310	227	0.35	0.98
$35^0\ S$	14.1	3	353	248	0.29	1.01
$25^0\ S$	19.1	24	386	269	0.24	1.05
$15^0\ S$	23.1	43	408	271	0.23	1.02
$5^0\ S$	24.6	61	420	262	0.23	0.98
$5^0\ N$	24.9	63	420	252	0.25	0.94
$15^0\ N$	24.3	46	408	264	0.24	0.99
$25^0\ N$	19.6	16	386	270	0.26	1.05
$35^0\ N$	13.0	-3	353	247	0.31	1.02
$45^0\ N$	6.2	-27	310	225	0.36	0.99
$55^0\ N$	0.4	-55	262	210	0.41	0.98
$65^0\ N$	-5.2	-81	216	198	0.46	0.98
$75^0\ N$	-13.4	-106	182	184	0.57	1.00
$85^0\ N$	-18.8	-127	169	183	0.67	1.07

Table 2: Components of the heat transport used in the calibrating and the diffusion coefficients estimated for atmospheric sensible and latent heat : F_s and F_l are the sensible and latent heat transports in the atmosphere, respectively, F_o is the oceanic heat transport from the ocean model, and the last two columns show the diffusion coefficients for atmospheric sensible and latent heat, respectively.

Latitude *Degree*	F_s $10^{15}\,W$	F_l $10^{15}\,W$	F_o $10^{15}\,W$	F $10^{15}\,W$	K_s WK^{-1}	K_l WK^{-1}
$90^0\,S$	0.00	0.00	0.00	0.00	0.0000	0.0000
$80^0\,S$	-0.35	-0.01	0.00	-0.36	0.1689	0.0970
$70^0\,S$	-1.48	-0.04	0.00	-1.52	0.2400	0.0615
$60^0\,S$	-2.65	-0.42	-0.07	-3.14	0.3516	0.1904
$50^0\,S$	-3.05	-1.51	-0.11	-4.67	0.4517	0.4765
$40^0\,S$	-3.04	-2.36	-0.06	-5.46	0.5018	0.5630
$30^0\,S$	-3.92	-1.39	-0.03	-5.34	0.6195	0.2349
$20^0\,S$	-4.80	0.44	-0.02	-4.38	0.8637	-0.0650
$10^0\,S$	-4.42	1.87	0.02	-2.53	2.0777	-0.6214
0^0	-1.67	1.33	0.52	0.18	3.4376	-1.8451
$10^0\,N$	3.06	-1.15	1.04	2.95	3.2190	-0.8219
$20^0\,N$	4.19	-0.33	1.09	4.95	0.6572	-0.0406
$30^0\,N$	3.40	1.16	1.02	5.58	0.4040	0.1499
$40^0\,N$	3.02	1.55	0.91	5.48	0.3988	0.3303
$50^0\,N$	3.10	0.87	0.66	4.63	0.5724	0.3830
$60^0\,N$	2.71	0.21	0.32	3.23	0.6567	0.1565
$70^0\,N$	1.61	0.08	0.01	1.71	0.3902	0.1061
$80^0\,N$	0.44	0.04	0.00	0.49	0.3213	0.3066
$90^0\,N$	0.00	0.00	0.00	0.00	0.0000	0.0000

3 Experiments

In the preceding section the atmospheric model has been tuned completely to reproduce present climatologies of surface air temperature and freshwater flux. The consistent climatologies of the climate system will be refered to as the control climate to which solutions from other experiments will be compared. It should be kept in mind that the ice-albedo factor did not enter the tuning procedure because the planetary albedo was taken from the observations. The factor is very important because it controls the positive feedback mechanism included in EBMs. Thus we would like to check the influence of the factor on model climate associated with the two versions of the model. Based on an analysis of the model's responses to a specified perturbation, a most reasonable value of f will be chosen to carry out further stability and sensitivity tests. In the analysis we took AGCM's responses as reference to choose the feedback factor used. Note that in all experiments to be described the oceanic heat transport shown in Table 2 will be used.

As described in the previous section, the model is governed by a non-linear, parabolic PDE for the temperature as a function of time and latitude, given the parameterizations involved. The main nonlinearity is due to the ice-albedo feedback. The governing equation is treated as an initial-value problem with boundary conditions that the heat transport vanishes at the poles. The meridional grid spacing is chosen to be 10^0 of latitude from pole to pole. The leap-frog scheme is used to solve the equation numerically. The time step of the integration, if not specifically mentioned, is one day. The diagnostic equation for the freshwater flux is solved with centred space differences for the meridional temperature gradient.

3.1 Effects of f

An external perturbation simulating a doubling of the atmospheric CO_2 is employed to study the response of model climates for different values of f. Because the only variable of the model is the temperature, the sensitivity refers to the temperature changes. Furthermore, we investigate the stability of the model with respect to different initial conditions for a range of the ice-albedo feedback factors f.

3.1.1 Version 1

We shall first examine the model sensitivity under an external perturbation of an uniform increase in net radiation of $+4\ Wm^{-2}$. Such an increase is characteristic of the global warming due to a doubling of the atmospheric CO_2 (Lal and Ramanathan, 1984). The integrations with different ice-albedo feedback factors f are started with the control climate as initial condition. It is found that a new equilibrium is generally reached after a few years. Figure 4 shows the changes in the temperature of the equilibrium response of the model to the perturbation with six selected ice-albedo feedback factors ranging from 0 to 0.010.

It is seen that the main difference among all the experiments appears in middle and high latitudes, ranging from 40 $^0\frac{S}{N}$ to 60 $^0\frac{S}{N}$. The maximum increase occurs at about 50 $^0\frac{S}{N}$ where the ice-albedo feedback seems to be most efficient. The almost uniform increase in the tropics is due to the parameterization of the albedo (see equation 27) that eliminates the feedback at temperatures above 283 K. The relatively small sensitivity polarward of around 75 $^0\frac{S}{N}$ can be explained by high albedos and small insulation there. Since the atmospheric heat transport is fixed, local temperature change is solely determined by change in net radiation which is associated with the ice-albedo effect. So a change of the temperature in a latitude zone is simply local, having no influence on the temperature change in another latitude zone. It is also shown by Figure 4 that the greater f is, the stronger the increase in temperature in middle and high latitudes will be.

To choose an appropriate value of f for the model, we take a look at some similar experiments carried out with AGCMs. The increases in global mean temperature of our model are 1.8, 2.0, 2.2, 2.7, 3.2, 3.8 K for f =0, 0.002, 0.004, 0.006, 0.008, 0.010 respectively, whereas AGCMs predict an increase ranging from 1.3 to 7 K (Dickinson, 1986) with a most likely range of 1.4–4.4 K (Mitchell, 1989). This implies that f =0.04–0.006 seems to be a good choice for the model to produce a comparable global sensitivity to most AGCMs.

However, caution must be taken when comparing results from AGCMs to that of the EBM since additional feedback mechanisms exist in AGCMs. Thus, we believe that it is necessary to isolate the ice-albedo effect in AGCMs for an approximate comparison with the EBM with regard to the feedback strength.

To discuss the global sensitivity of different climate models to external perturbations, a globally averaged model is usually used to assess feedbacks qualitatively (see *e.g.* Lashof, 1989). This model is formulated as follows:

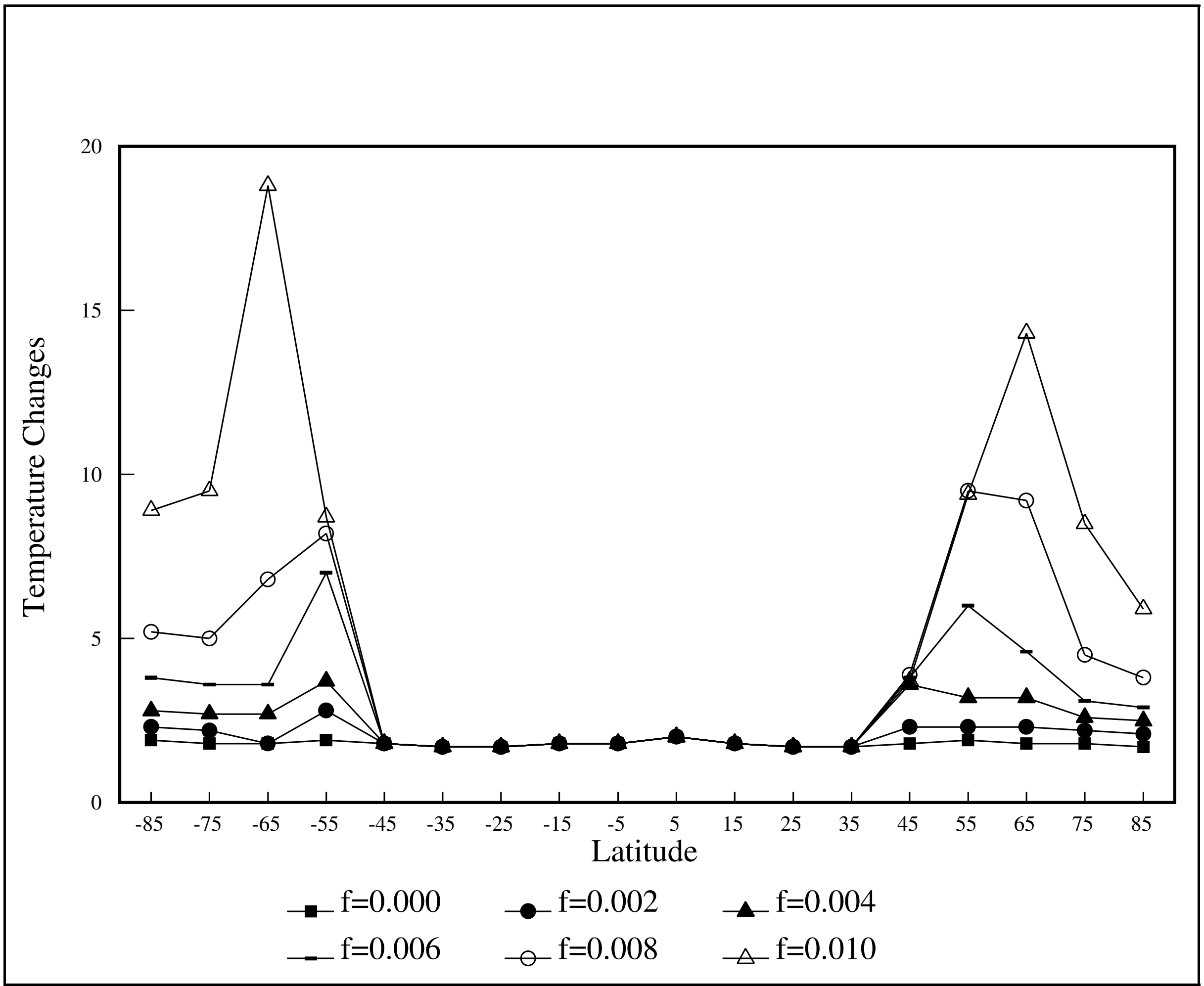

Figure 4: Model version 1 responses to a doubling of CO_2 with different ice-albedo feedback factors. Temperature changes are expressed by the difference between equilibrium temperature distribution due to the doubling of CO_2 and that of the control climate in K.

$$C\,\frac{\partial(\Delta T_0)}{\partial t} + \lambda(\Delta T_0) = \Delta R_t \tag{41}$$

where C is the heat capacity of the climate system, ΔT_0 is the change in global mean surface air temperature, ΔR_t is an externally prescribed change in net radiation, and λ is the feedback parameter of the internal dynamics of the system. As we are only concerned with the equilibrium response, equation (41) can be further simplified,

$$\Delta T_0 = \frac{\Delta R_t}{\lambda}. \tag{42}$$

As pointed out by Dickinson (1986), λ is an overall climate system sensitivity factor which includes the sum of all contributing feedback factors which are operative in the system. λ is a convenient measure of the strength of individual feedbacks because of its additive nature. It is possible, by carrying out experiments with certain feedbacks switched on or off, to identify individual feedback parameters due to different mechanisms.

To assess the ice-albedo feedback in the model, we first estimate a reference value (λ_0) for a case without the feedback ($f = 0$). The global temperature increase in the CO_2-doubling experiment with $\Delta R_t = 4\,Wm^{-2}$ is 1.8 K, implying from (42) that $\lambda_0 = 2.22$. Note that λ_0 includes black-body (λ_B) and long-wave water vapour feedbacks (λ_W). λ_B can be estimated by

$$\lambda_B = 4\sigma T_e^3 = 3.75\ Wm^{-2}K^{-1} \tag{43}$$

where σ is the Stefan-Boltzmann constant, and $T_e = 255\ K$ is the earth's effective radiative temperature. Then,

$$\lambda_W = \lambda_0 - \lambda_B = -1.53\ Wm^{-2}K^{-1} \tag{44}$$

λ_W has been estimated by Mitchell (1987) from CO_2-doubling experiments using both radiative-convective models and AGCMs. These experiments indicate that λ_W ranges from -1.4 $Wm^{-2}K^{-1}$ to -1.8 $Wm^{-2}K^{-1}$, which agrees well with the above result.

With help of λ_0 we can estimate the contribution of the ice-albedo feedback (λ_α) to the total feedback parameter λ with different feedback factors f in our model. It is found that λ_α ranges from -0.22 $Wm^{-2}K^{-1}$ to -1.17 $Wm^{-2}K^{-1}$ as f varies from 0.002 to 0.010.

One dimensional EBMs developed so far show λ_α ranging from -0.3 $Wm^{-2}K^{-1}$ (Lian and Cess, 1977) to -0.8 $Wm^{-2}K^{-1}$ (Sellers, 1969), while AGCMs have an even wider range of the feedback parameter. For example, an experiment carried out by Washington and

Meehl (1983) indicates $\lambda_\alpha \approx 0.0\ Wm^{-2}K^{-1}$, whereas in another experiment they found $\lambda_\alpha \approx -0.9\ Wm^{-2}K^{-1}$ (Washington and Meehl, 1984). With an interactive ocean, Spelman and Manabe (1984) find $\lambda_\alpha \approx -0.45\ Wm^{-2}K^{-1}$ which is somehow a representative value for many AGCM experiments (Mitchell, 1989).

Because the feedback parameter depends very much on sea ice and we will couple this model to an OGCM, we chose $f = 0.004$, which corresponds to $\lambda_\alpha \approx -0.40\ Wm^{-2}K^{-1}$. Another reason why we prefer a small value of f in version 1 is that it produces too strong local sensitivity at middle latitudes.

Our model is too sensitive to give a reasonable response once f exceeds 0.008. In other words, the upper bound of f implied by the sensitivity experiments is about 0.008.

To investigate the effect of the feedback factor on stability, we first carried out some time integrations from initial conditions close to the control climate state. Time-dependent solutions of the initial-value problem will converge as $t \to \infty$ to a steady state which is near the control climate if it is stable. The results show that solutions converge with perturbations as large as $\pm 10\ ^0K$ provided $f < 0.010$. This finding confirms that the model is stable when f ranges from 0 to 0.010.

Since the perturbations employed are small, the stability proved is linear stability. To consider the nonlinear stability we need to look at how solutions evolve when perturbations far from the control climate are applied.

If a nonlinear process is invoked, the system may have multiple equilibria. Indeed, it is well known that many time-independent EBMs have three (*e.g.* North, 1975) or even more (Ghil, 1976) steady-state solutions when the ice-albedo effect is included. To find out if our model also possesses this characteristic, we started the integration with initial conditions far away from the control climate. The model is found to be very stable to positive temperature perturbations. However, an additional solution besides the present climate appears if negative perturbations in the initial conditions are more than 20 K, provided $f > 0.005$. The second solution is characterised by very low temperatures everywhere, which will be refereed to as an ice-covered earth solution. However, the ice-covered earth solution disappears for $f < 0.005$, no matter how strong the perturbation is. For $f < 0.005$, the model has only one unique solution which is the present climate. This state is very stable.

It is of interest to note that the overall feedback parameter λ is also a very useful parameter in expressing the uncertainties of climate models. With the $2 \times CO_2$ experiment AGCMs show the best estimate of a total feedback parameter from 0.9 to 2.8 $Wm^{-2}K^{-1}$. Uncertainties in the simulation of the cloud-radiation and ice-albedo feedbacks are responsible for this wide range of λ. The total feedback parameter in our model is 1.8 $Wm^{-2}K^{-1}$, well in the range given above.

Finally we would like to show the diagnosed freshwater flux associated with the $2 \times CO_2$ experiment in Figure 5. We see that the freshwater flux is altered most significantly in middle latitudes, although there also appears a remarkable change near the equator. There is a general reduction of the flux within the latitude zone from 50 ^0S to 40 ^0N except near the equator, whereas a significant increase can be observed near 55 ^0S and 45 ^0N.

A similar AGCM experiment carried out by Manabe and Wetherald (1980) (hereafter referred to as MW) shows a decrease in the flux equatorward of about 40 $^0\frac{N}{S}$ and an increase polarward of about 40 $^0\frac{N}{S}$. The increase within the narrow latitude zone shown by our model is attributable to the most significant temperature change predicted there.

As the atmospheric heat transport is fixed, the diffusion parameterization for the sensible heat transport implies that change in the latent heat transport is also linked to the meridional temperature gradient. Therefore, the most remarkable increase of temperature around 50 $^0\frac{S}{N}$ results in the increased freshwater flux mentioned above.

3.1.2 Version 2

The same perturbation is also added to version 2 of the model. The equilibrium response of the model to the perturbation with f ranging from 0.00 to 0.010 is shown in Figure 6. Compared with the response in version 1 (shown in Figure 3), version 2 shows a much smoother change in the temperature with respect to latitude. Obviously this is due to the variable heat transport built in. While the great sensitivity in the vicinity of the ice line disappears, an evident polar amplifying effect is observed in Figure 6. This effect is more evident as the ice-albedo factor f increases. The increase in temperature around 5 ^0N appears to be larger than in the neigboring regions. This is due to the smallest value of CF found there. Note that $\partial I/\partial T_0 = CF \cdot B$, so CF really determines the local strength of the longwave radiation- water vapour feedback since B is constant. Taking into account that 5 ^0N is where the annual mean ITCZ is located, it may not be surprising that the

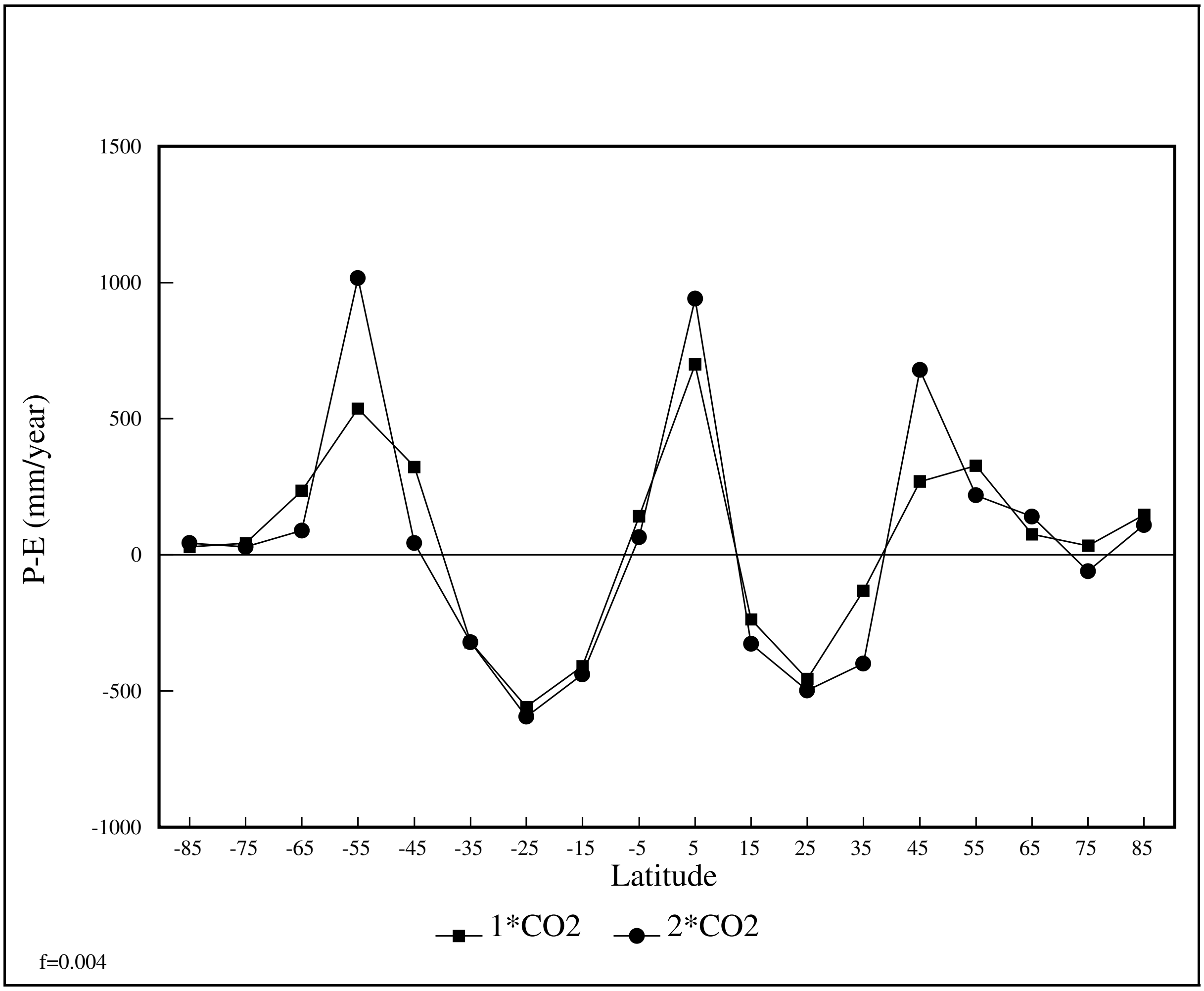

Figure 5: Freshwater fluxes in the control climate and in the experiment with the doubling of the atmospheric CO_2

greater sensitivity exists off the equator. Since the parameterization of the albedo is as in version 1, the polar amplifying effect found in version 2 may be attributed to an additional feedback mechanism: transport-temperature feedback.

The increases in the global mean temperature of version 2 are 1.9, 2.0, 2.2, 2.5, 2.9, 3.1 K for f =0.00, 0.002, 0.004, 0.006, 0.008, 0.010 respectively. Although the local sensitivity of version 2 differs remarkedly from version 1, the global sensitivities of the two versions show good agreement. Version 2 shows a slightly smaller global sensitivity for $f \geq 0.006$, indicating that the transport-temperature feedback is a negative feedback in this case. Version 2 produces a much smoother latitudinal temperature variation than version 1. The smoother temperature variation will not cause a problem for the diagnostics of the freshwater flux as in version 1. Contrary to the rather small value of f in version 1, we can use $f = 0.006$ in version 2.

Note that the only difference between the two versions is, in terms of the feedback analysis, that version 2 has one more mechanism operating. The effect of the feedback on the global sensitivity can be assessed by a feedback parameter λ_T. As discussed above, λ_T is simply the difference between the two total feedback parameters of the two versions with an equal λ_α. For $f = 0.006$ the total feedback parameter $\lambda_1 = \frac{4}{2.5}\frac{W}{m^2K}$ and $\lambda_2 = \frac{4}{2.7}\frac{W}{m^2K}$ for version 1 and 2, respectively. This results in an estimate of $\lambda_T = 0.12\,Wm^{-2}K^{-1}$ for the total heat transport. From the experiments with version 1 we estimate $\lambda_\alpha = -0.74\,Wm^{-2}K^{-1}$ for $f = 0.006$.

The polar amplifying effect in version 2 is very interesting because it reproduces an important feature of the global warming commonly found in AGCMs. This warming in AGCMs has been intepreted as due to positive lapse rate and ice-albedo feedbacks at high latitudes. However, the parameterization of heat transport associated with the ice-albedo feedback in our model appears to be responsible for the amplification.

MW point out that increased latent heat transport in a warmer climate contributes to the reduction in meridional temperature gradient near the surface. In Figure 7 the latent transports in response to the doubling of CO_2 and that from the control climate are shown. The latent heat transport increases at all latitudes in our model, which is due to the exponential temperature dependence of the saturation water vapour pressure with warming (see equation 35). The maximum increase appears near the equator, because $\partial q_s/\partial T_0$ increases with increasing temperature.

It is expected that the increased latent heat transport will result in an increase in

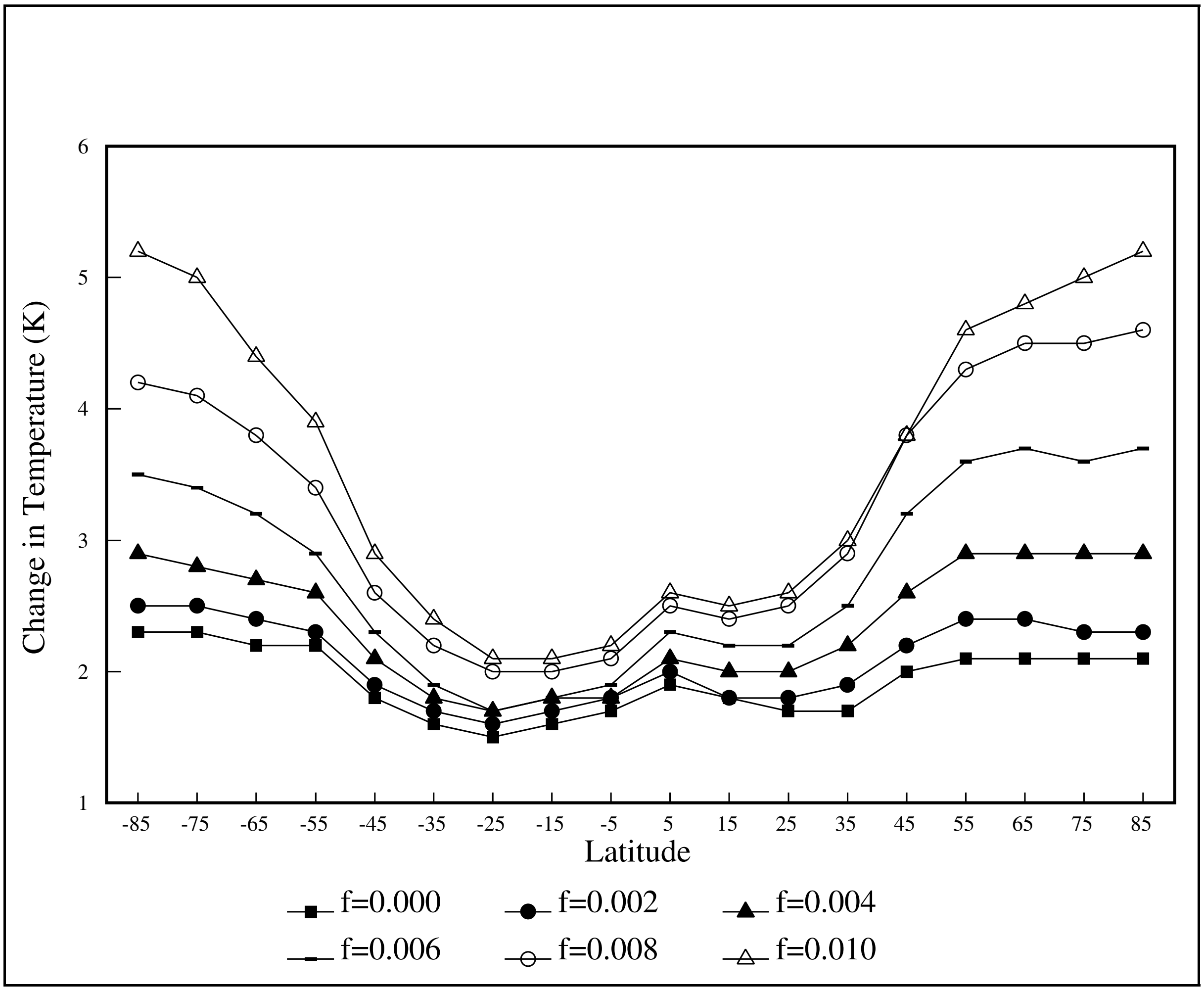

Figure 6: Model version 2 responses to a doubling of CO_2 with different ice-albedo feedback factors. Temperature changes are expressed by the difference between the equilibrium temperature distribution due to the doubling of CO_2 and that of the control climate.

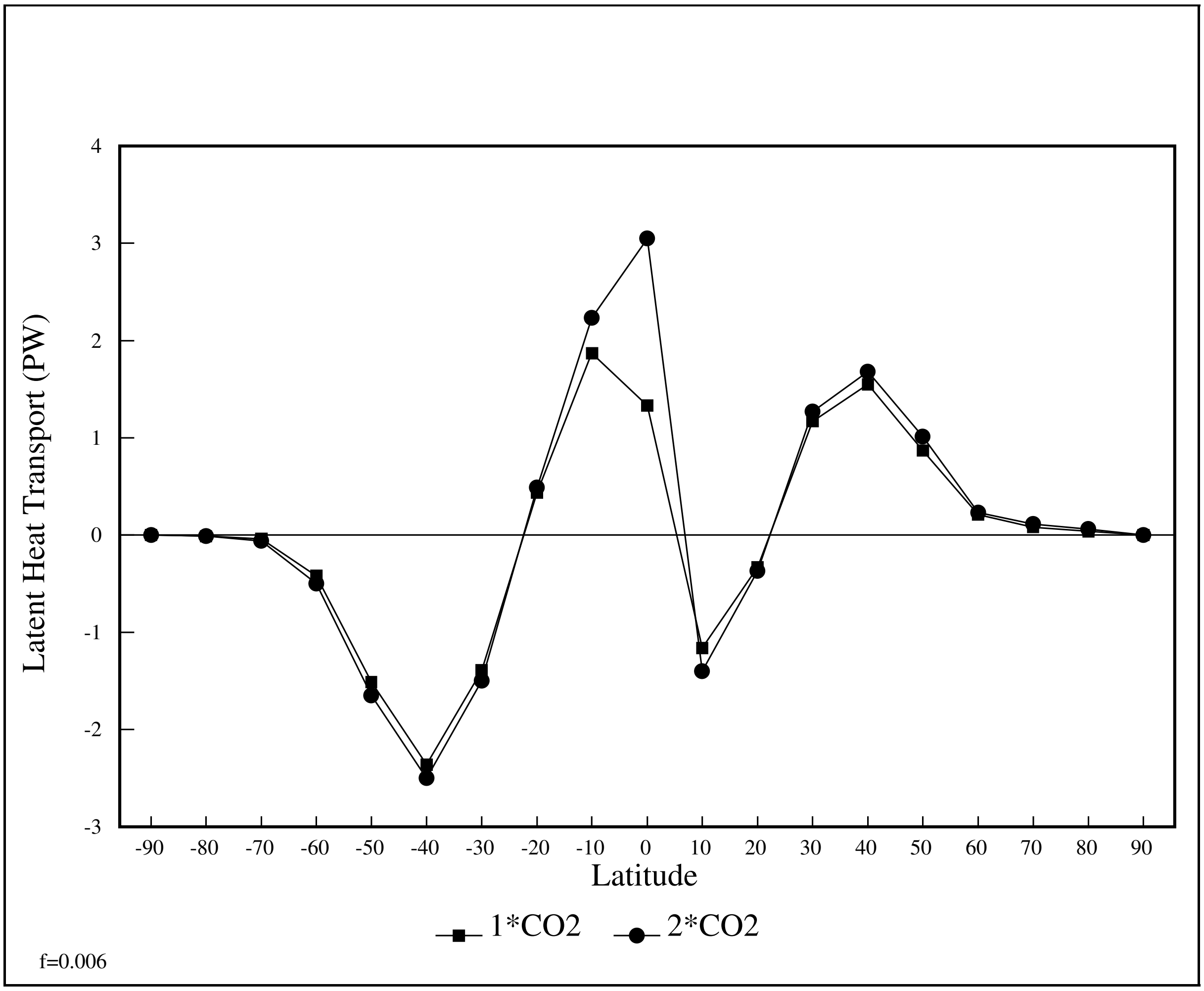

Figure 7: Latent heat transports due to a doubling of the atmospheric CO_2 and that from the control climate.

amplitude of the freshwater flux. The diagnosed freshwater flux associated with the $2 \times CO_2$ experiment and that from the control climate are displayed in Figure 8. The freshwater supply to the ocean will increase at middle and high latitudes and near the equator, whereas a general decrease is found at subtropical latitudes. This result is very similar to that of MW.

On the other side, as the meridional temperature gradient decreases in the warmer climate, the sensible heat transport which is proportional to the gradient will decrease. From Figure 9 we can see that to a large extent the increased latent heat transport is compensated by the reduced sensible heat transport in our model, as is found in MW.

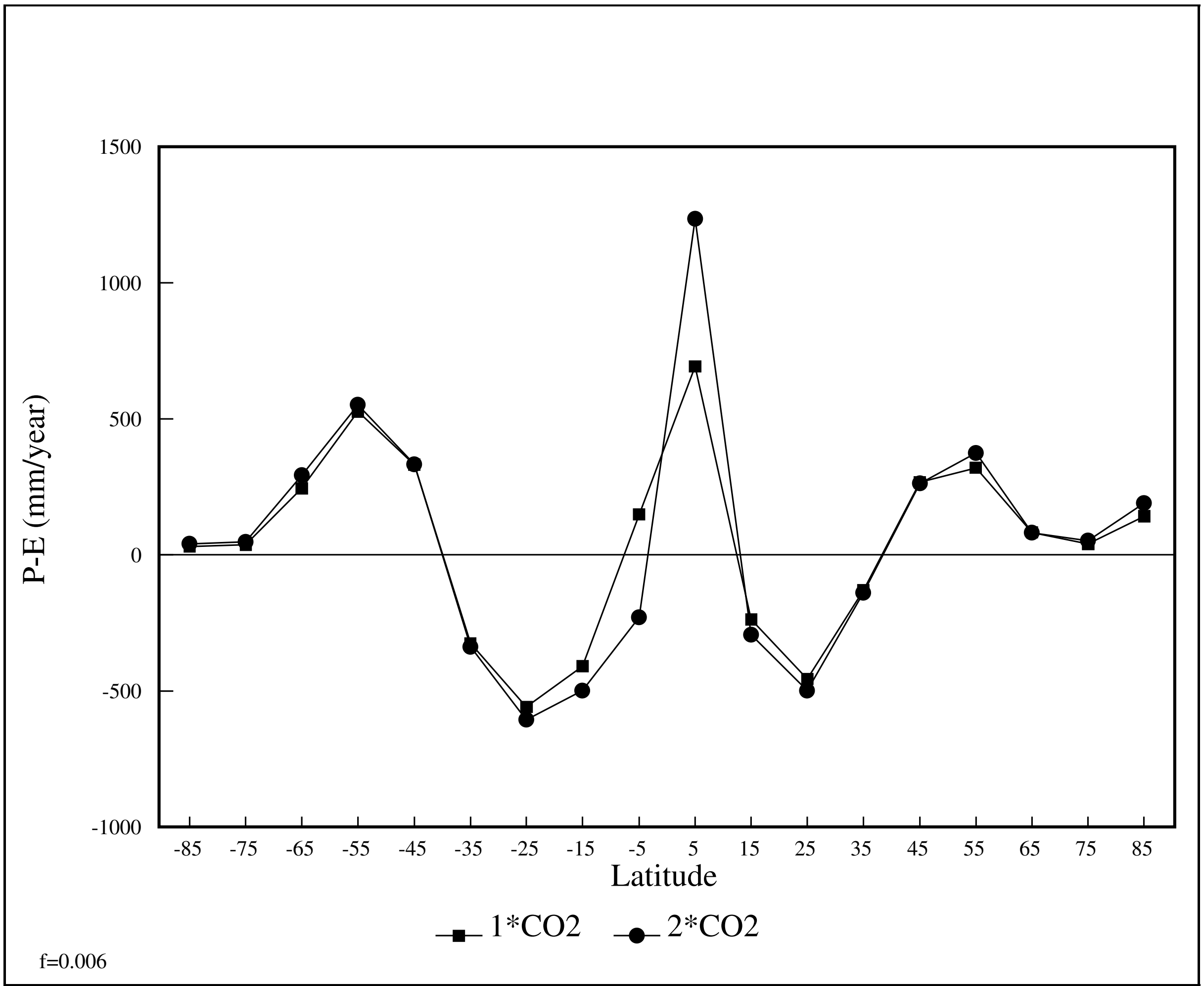

Figure 8: Freshwater fluxes in the control climate and in the experiment with the doubling of the atmospheric CO_2.

Actually the total heat transports in the control and warmer climates shown by Figure 10 reveals that the change is generally very small, implying that the atmospheric heat transport is almost unchanged under the global warming. However, a closer inspection of the Figure shows that the atmospheric transport in the warmer climate is reduced, especially around middle latitudes. To see the decrease more clearly, we plot the difference in the atmospheric transport between the warmer and control climates in Figure 11.

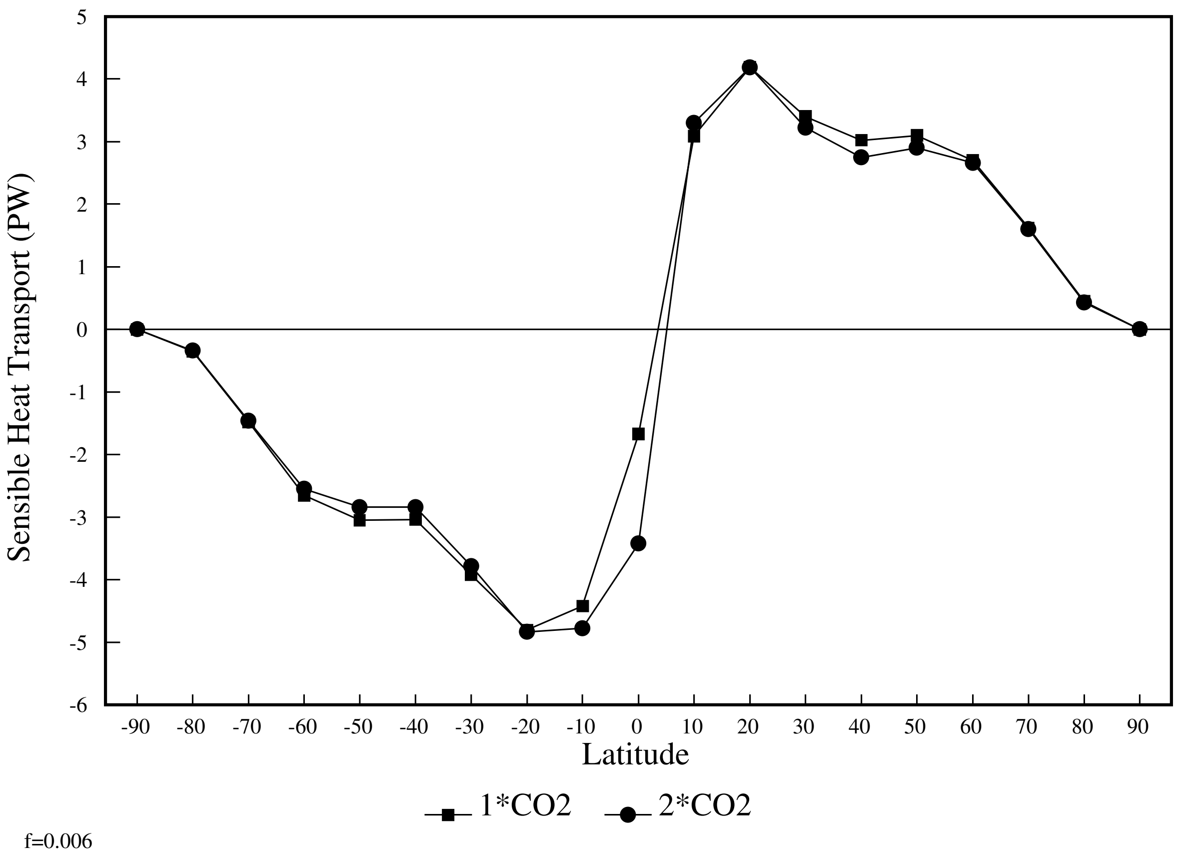

Figure 9: Sensible heat transport in the control climate and in the experiment due to a doubling of the atmospheric CO_2.

The polarward atmospheric heat transport is reduced in the warmer climate almost everywhere, though the change is small. While the decrease at middle and high latitudes agree well with the results of MW, the decrease at low latitudes is just opposite to what is found by MW. The net increase in the atmospheric transport at low latitudes found by MW is due to the fact that the amplitudes of the latent and sensible heat transports are almost equal in their model, implying that the hydrological cycle in MW's model is very strong. In our model, however, the sensible heat transport is about three times larger than the latent transport. Therefore, the reduction in the sensible transport plays a dominant role, resulting in finally the decrease in the atmospheric transport.

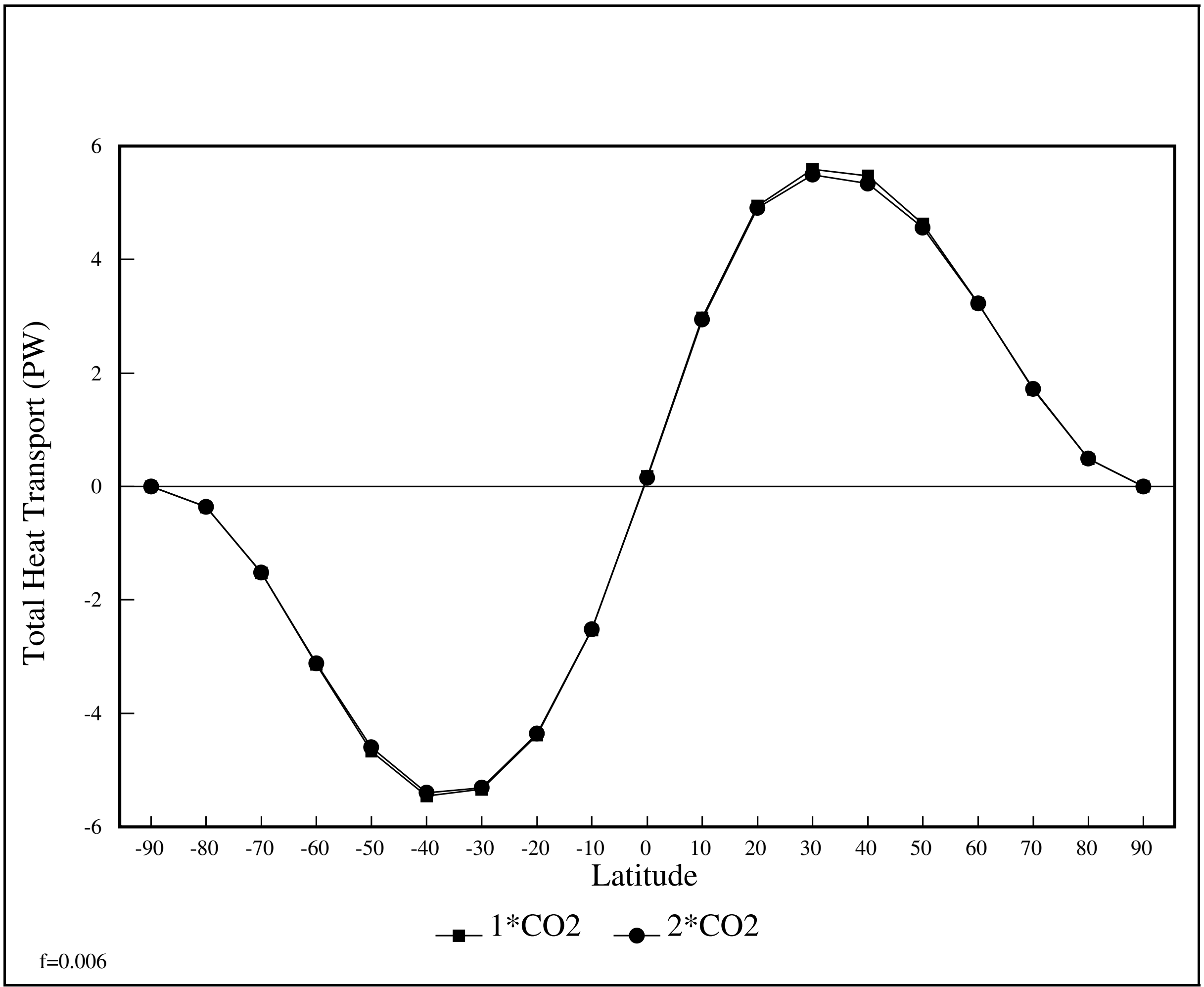

Figure 10: Comparison between the total heat transports in control climate and that due to a doubling of the atmospheric CO_2.

It is interesting to notice that version 2 predicts a larger increase in the temperature at high latitudes under the global warming even though the atmospheric heat transport is reduced. This result indicates that it is the combined effect of the ice-albedo and transport-temperature feedbacks that causes the polar amplification.

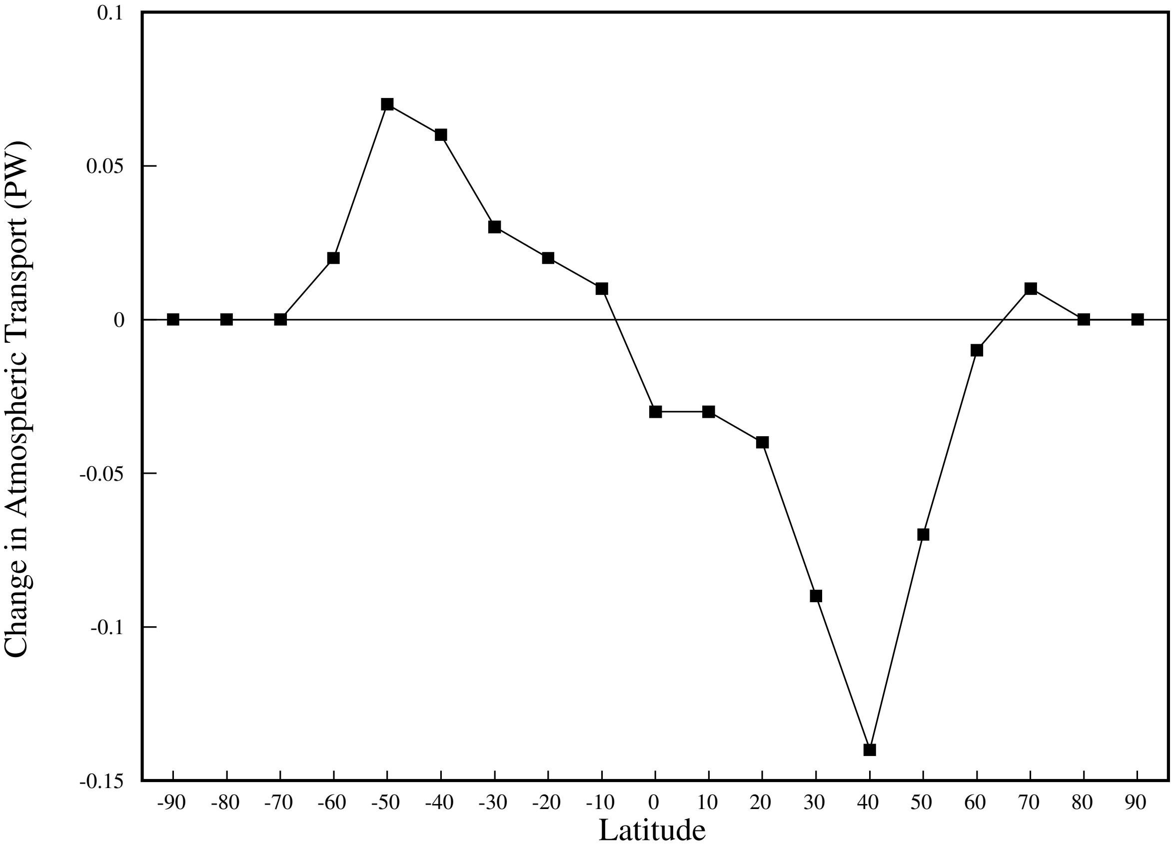

Figure 11: Changes in the atmospheric heat transport due to a doubling of the atmospheric CO_2.

3.2 Standard sensitivity tests

Traditionally the sensitivity of EBM is studied and expressed in terms of a parameter which is a measure of the change in global average temperature due to 1% change in the solar constant, since the model sensitivity to any other perturbation is roughly proportional to this parameter (North *et al.*, 1981). Two standard sensitivity experiments are performed here to show the model sensitivity to changes in the incoming solar radiation.

3.2.1 Version 1

The model responses to an increase and decrease of 1% in the solar constant are shown in Figure 12 and Figure 13 for temperature changes and freshwater changes respectively.

The changes in temperature decrease with increasing latitude, except at middle latitudes where the ice-albedo feedback amplifys the changes. This is because the incoming solar radiation is smaller and the albedo is higher at higher latitude.

As discussed above, the freshwater flux varies according to the change in the meridional temperature gradient. Thus significant changes occur at middle latitudes and near the equator.

3.2.2 Version 2

Figure 14 and Figure 15 show the results of perturbing the model with a step function of $\pm 1\%$ solar constant increase after equilibrium has been established.

Compared with the result of version 1, temperature changes are smoothed out. Also, the polar amplification can be observed, although the absolute value of the perturbations decreases with increasing latitude. The smoother temperature distribution results in a more regular change in the freshwater flux. The pattern of the response in the freshwater flux in the case of $+1\%$ change in the solar constant resembles that in the $2\times CO_2$ experiment. As the change in incoming solar radiation is latitude-dependent, the response of version 2 seems to be fairly independent on local perturbation.

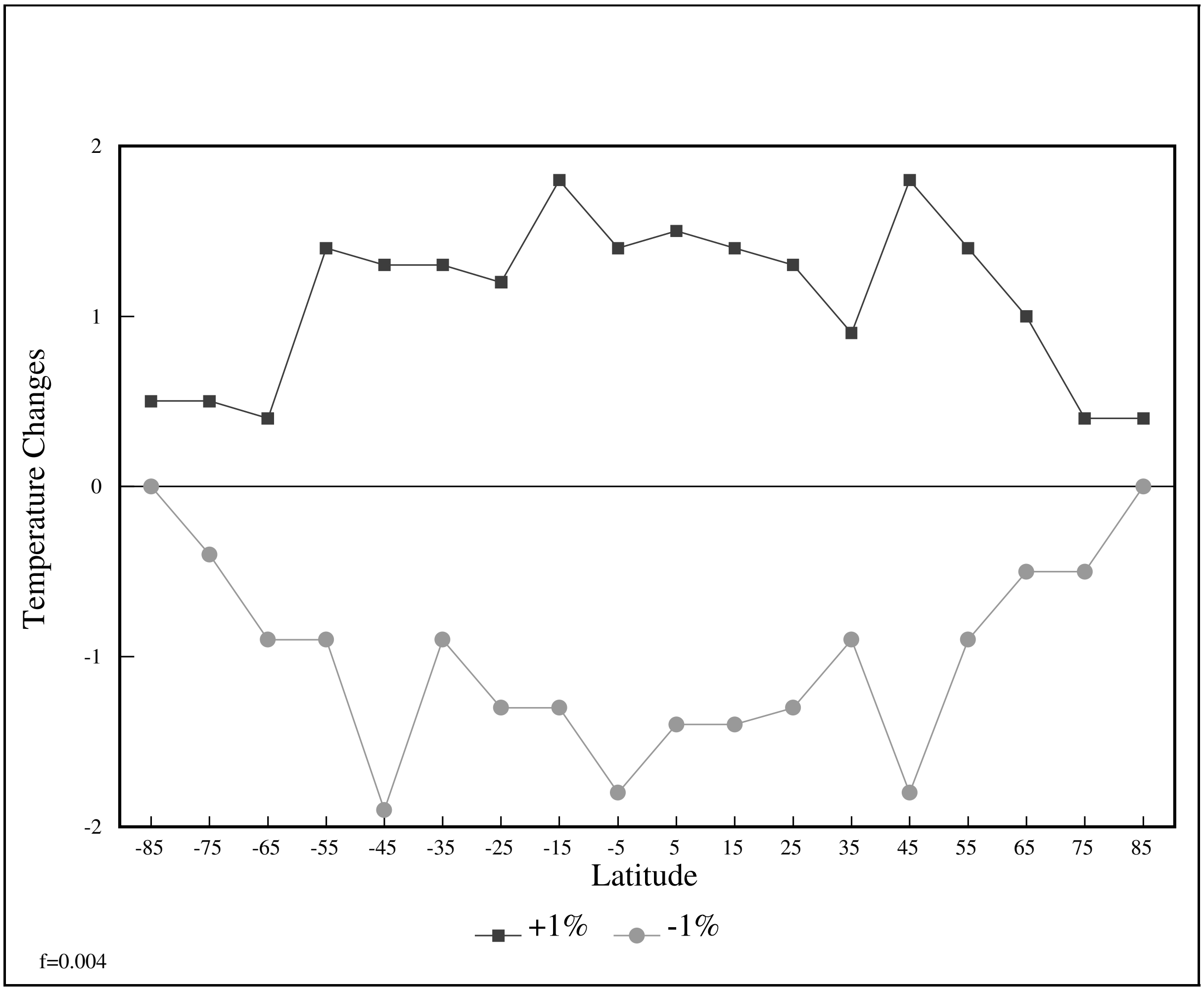

Figure 12: Changes in the surface air temperature due to the perturbations in the solar constant.

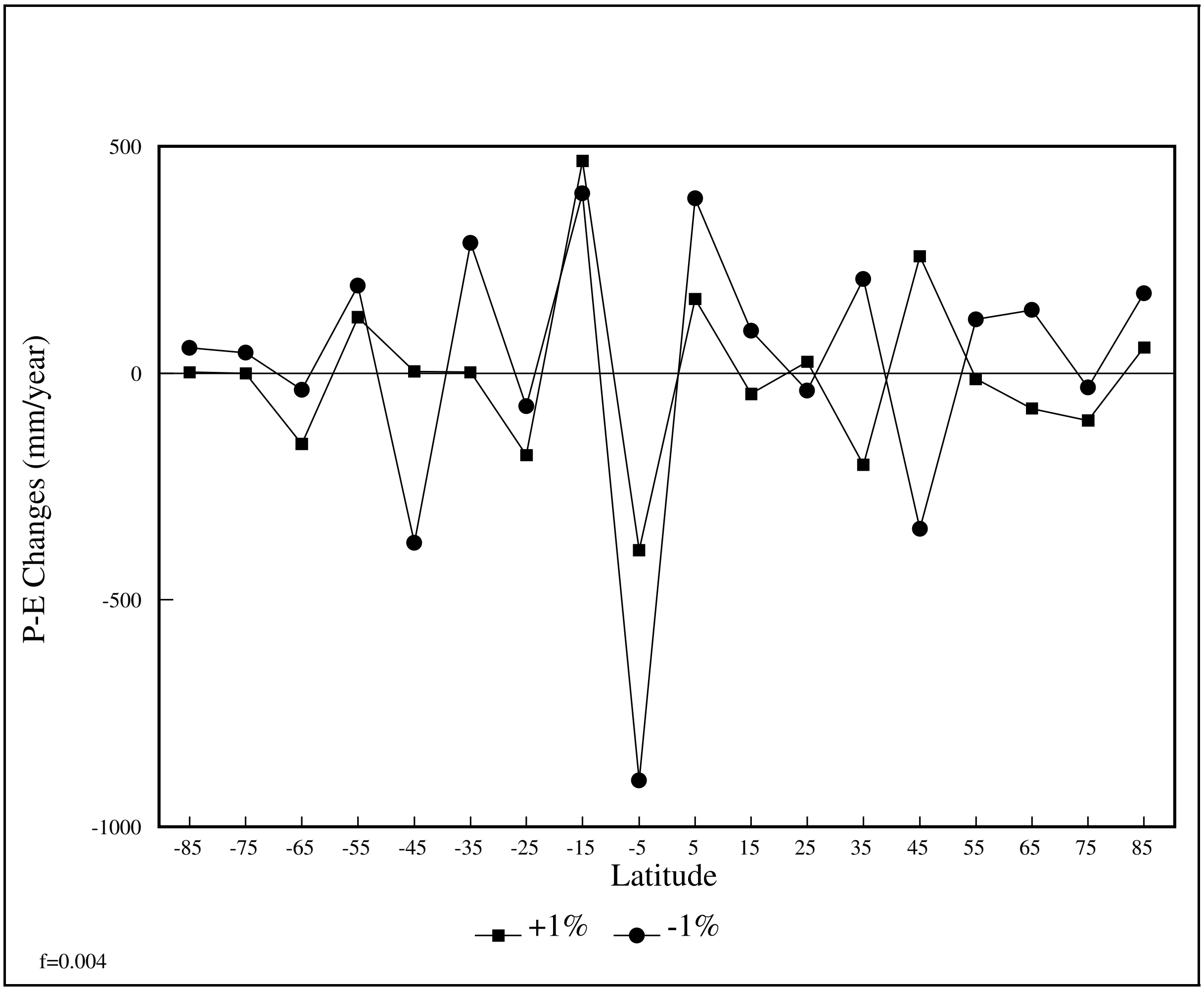

Figure 13: Changes in the freshwater flux due to the perturbations in the solar constant

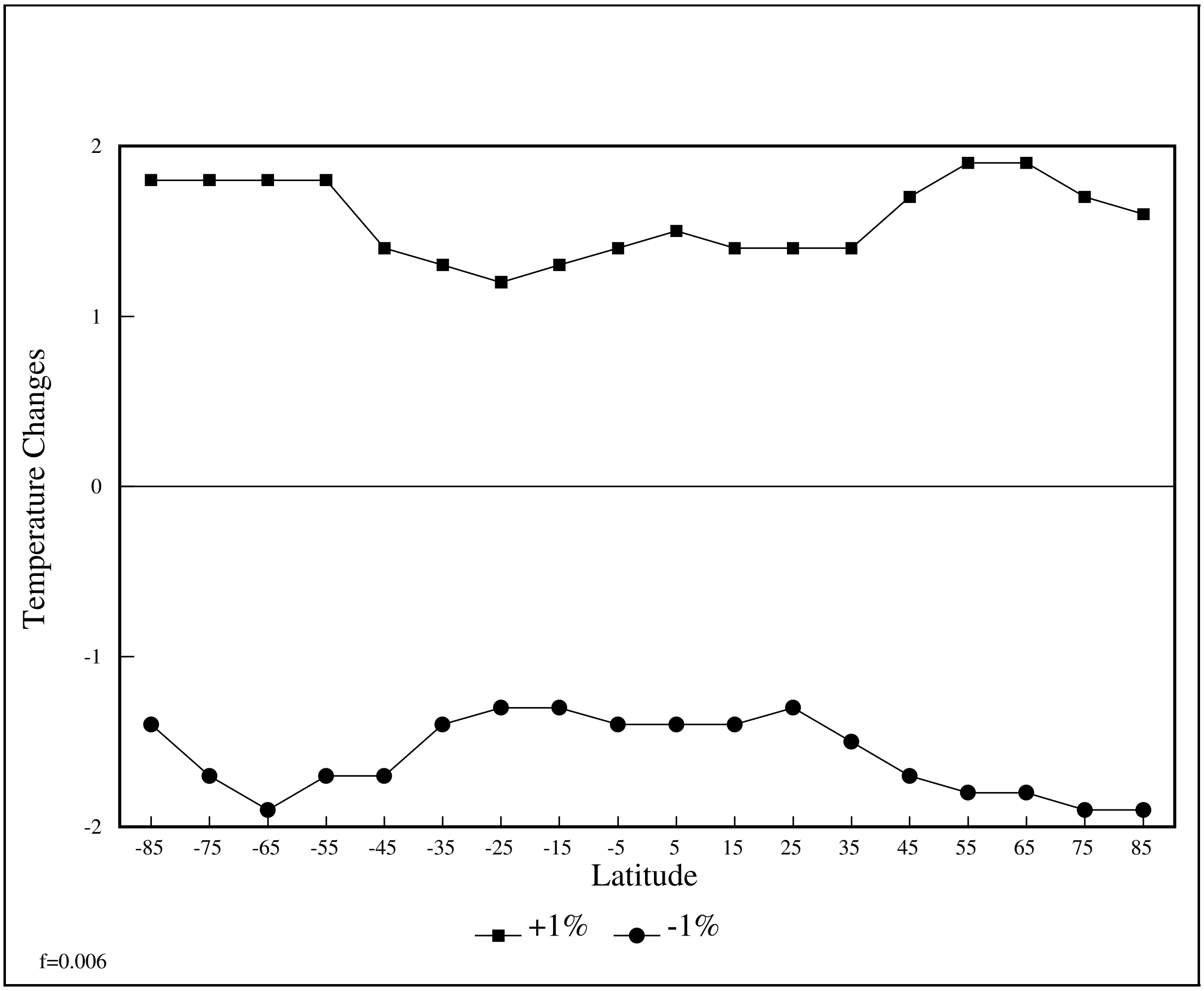

Figure 14: Changes in the surface air temperature due to the perturbations in the solar constant

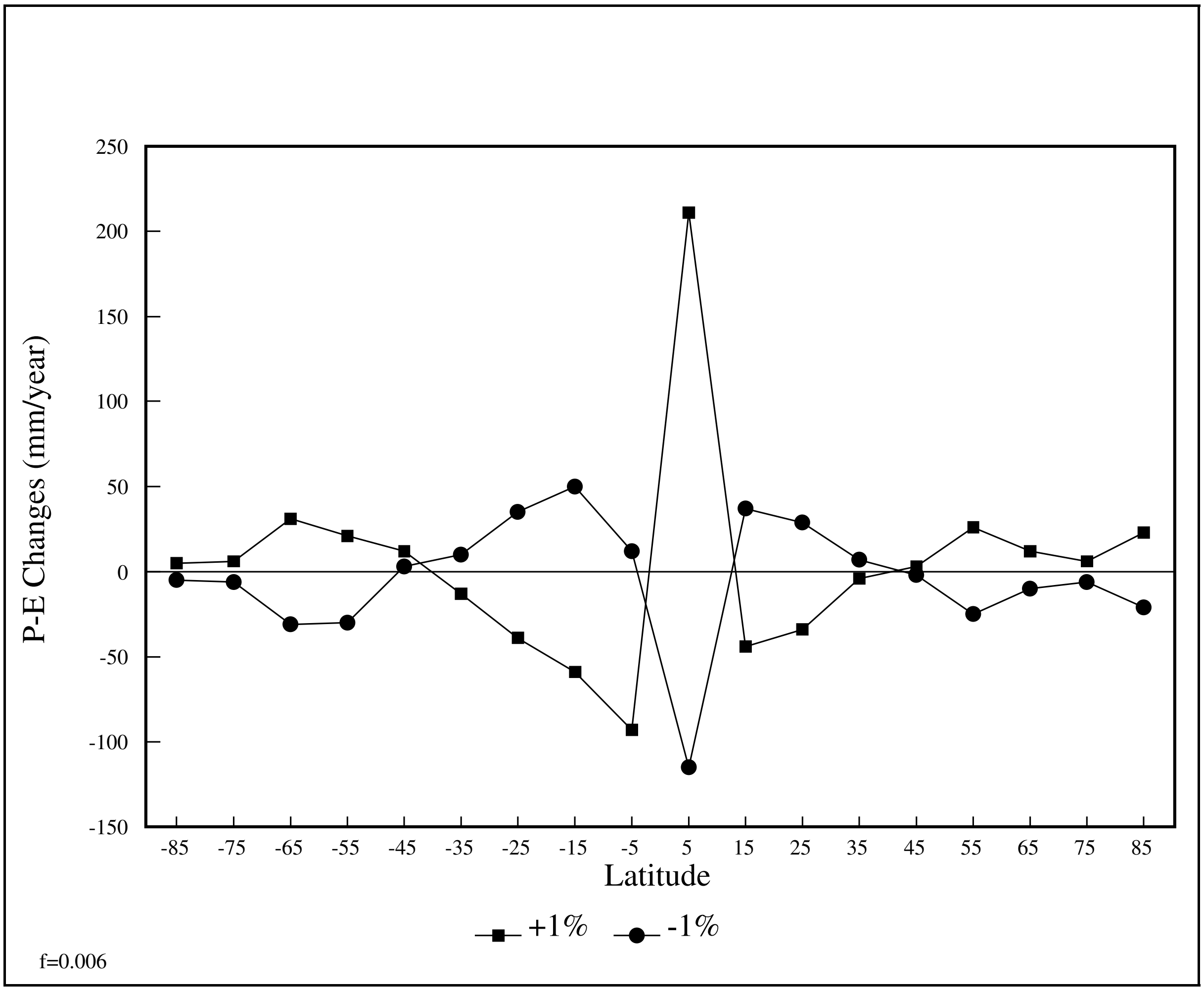

Figure 15: Changes in the freshwater flux due to the perturbations in the solar constant

4 Summary

The main purpose of this report has been to develop an atmospheric model to be used for coupled atmosphere-ocean modelling problems. Although the ocean component must be considered in the development of the model, this report has been restricted to a presentation of the atmospheric component of the climate system, its simulation of the present climate, and its sensitivity to perturbations in a decoupled mode. The basic idea was to keep the model as simple as possible since this is the first step to treat the problem. The model has two versions, which differ in the parameterization of the components of the heat transport within the ocean-atmosphere system.

We have derived the governing equation of the atmospheric model based on the first law of thermodynamics in section 2, where a detailed description of the related parameterizations is also given. The main assumptions inherent in the derivation are

1. The contribution of kinetic energy to the total energy budget can be ignored.
2. Planetary albedo may be parameterized in terms of surface air temperature and the ice-albedo feedback factor.
3. Outgoing radiation may be parameterized in terms of surface air temperature and a latitude-dependent consistent factor.
4. The vertical gradient of potential temperature in the tropospheric atmosphere is constant with respect to height and can be parameterized in terms of the surface air temperature. Based on the parameterization of Rennick, two distinct thermal inertias, as felt by the surface air temperature, are found. They are $5.74 \times 10^6 \; Jm^{-2}K^{-1}$ at latitudes equatorward $50^0 \frac{N}{S}$ and $3.99 \times 10^6 \; Jm^{-2}K^{-1}$ over the rest of the globe, respectively.
5. Internal variation of atmospheric moisture content is to be neglected so that the latent heat transport may be related to the freshwater flux at the ground.
6. The sensible heat transport in the atmosphere may be expressed by a diffusion process and the diffusion coefficient does not change.
7. In version 1 of the model the total heat transport remains constant and the latent heat transport is diagnosed as a residual. In version 2 the atmospheric moisture transport is treated as a diffusion process. We also made the assumption in version 2 that the relative humidity does not change.

The stability and sensitivity of the model are closely examined in section 3 by some experiments in which either internal or external parameters of the model are altered. In particular, the effect of the ice-albedo feedback on solutions of the two versions of the model is studied with a $2 \times CO_2$ experiment. The results may be summarised as follows:

1. It appears that the largest uncertainty for the sensitivity of global mean temperature to external and internal perturbations is the magnitude of the ice-albedo feedback factor. On the other side, the parameterizations for the heat transport have great impact on local sensitivity.

2. The ice-albedo feedback not only strongly affects the sensitivity and stability of the model, but also controls the existence of multiple equilibrium solutions. We found that version 1 and 2 of the model are transitive to a large range of initial temperature perturbations as long as $f < 0.005$ and $f < 0.009$, respectively. Otherwise, two stable intransitive steady states are found: one for the present-day climate and another for an ice-covered Earth.

3. Based on the results of the $2 \times CO_2$ experiment, the feedback factors are chosen to be 0.004 and 0.006 for version 1 and 2 respectively, which correspond to ice-albedo feedback parameters λ_α of -0.40 and -0.74 $Wm^{-2}K^{-1}$ for version 1 and 2 respectively. As the feedback parameterss used are relatively small, a transition to an ice covered Earth is prevented.

4. The total feedback parameters of version 1 and 2, estimated with the $2 \times CO_2$ experiment, are 1.82 and 1.60 $Wm^{-2}K^{-1}$ respectively. The corresponding changes in global mean temperature are 2.2 and 2.5 K.

5. While the global mean temperature change under perturbation is nearly identical in the two versions of the model, the response with latitude varies considerably.

6. Although the experiments with version 2 show that the total heat transport under different forcings can be satisfactorily approximated as constant, the tiny variation of the transport does change the local responses significantly, especially those at middle and high latutudes, because of the ice-albedo feedback. Thus, the coupling between the transport and the feedback appears to be very important.

7. In terms of the predicted temperature and the diagnosed freshwater flux distribution, version 2 closely reproduces results from similar AGCM experiment. Hence, the application of version 2 will be prefered.

8. This EBM is appealing because of its simplicity to allow quick integrations and its ability to reproduce most important qualitative features of the climate variability found from AGCM simulations.

Although much work remains to be done before the extent to which this simple atmospheric model can help us in understanding the problems in ocean modelling can be assessed, we feel that the simple energy balance models have an important role to play in our developing knowledge of the coupling between the atmosphere and ocean.

Currently, the EBM is coupled to the OGCM at AWI. The results of the interactive experiments will be reported elsewhere.

References

[1] Bowman, K. P., Sensitivity of an energy balance climate model with predicted snowfall rates, *Tellus*, **37A**, 233-248, 1985.

[2] Bryan, F., High-latitude salinity effects and interhemispheric thermohaline circulations, *Nature*, **323**, 301-304, 1986.

[3] Carissimo, B. C., A. H. Oort, and T. H. Vonder Haar, Estimating the meridional energy transports in the atmosphere and ocean, *J. Phys. Oceanogr.* **15**, 82-91, 1985.

[4] Covey, C., Atmospheric and oceanic heat transport: simulations versus observations, *Climatic Change*, **13**, 149-159, 1988.

[5] Cox, M. D., A primitive equation, three-dimensional model of the ocean, GFDL Ocean Group Tech. Rep. No. 1, GFDL/NOAA, Princeton University, 1984.

[6] Dickinson, R. E., How will climate change?, The Greenhouse Effect, Climate Change and Ecosystems, edited by B. Bolin, B. R. Doos, J. Jaeger, and R. A. Warrick, *SCOPE Rep.*, 29, 206-270, 1986.

[7] Ghil, M., Climate stability for a Sellers-type model, *J. Atmos. Sci.* **33**, 3-20, 1976.

[8] Haney, R. L., Surface thermal boundary conditions for ocean circulation models, *J. Phys. Oceanogr.* **1**, 241-248, 1971.

[9] Harvey, L. D. Danny, A semianalytic energy balance climate model with explicit sea ice snow physics, *J. of Climate* **1**, 1065-1085, 1988.

[10] Holton, J. R., An Introduction to Dynamical Meteorology. Int. Geophysics. Ser., Vol. 23. Academic Press, 391 pp, 1979.

[11] Jentsch, V., An energy balance climate model with hydrological cycle: 1. Model description and sensitivity to internal parameters, *J. Geophys. Res.* **96**, 17,169-17,179, 1991.

[12] Jentsch, V., An energy balance climate model with hydrological cycle: 2. Stability and sensitivity to external forcing, *J. Geophys. Res.* **96**, 17,181-17,193, 1991.

[13] Lal, M., and V. Ramanathan, Effects of moist convection and water vapour radiative processes on climate sensitivity, *J. Atmos. Sci.* **41**, 2238-2249, 1984.

[14] Lashof, Daniel A., 1989, The dynamic greenhouse: Feedback processes that may influence future concentrations of atmospheric gases and climatic change. *Climatic Change*, **14**, 213-242.

[15] Lian, M. S. and R. D. Cess, Energy balance climate models: A reappraisal of ice-albedo feedback, *J. Atmos. Sci.* **34**, 1058-1062, 1977.

[16] Manabe, S. and K. Bryan, CO_2-induced change in a coupled ocean-atmosphere model and its paleoclimatic implications, *J. Geophys. Res.* **90**, 11,689-11,707, 1985.

[17] Manabe, S. and R. T. Wetherald, On the distribution of climate change resulting from an increase in the CO_2 content of the atmosphere, *J. Atmos. Sci.* **37**, 99-118, 1980.

[18] Marotzke, J. and J. Willberand, Multiple equilibria of the global thermohaline circulation, *J. Phys. Oceanogr.* **21**, 1372-1385, 1991.

[19] Mitchell, J. F. B., Climate sensitivity and past climates; Evidence from numerical studies, in *Abrupt Climatic Change*, edited by W. H. Berger and L. D. Labeyrie, 383-398, D. Reidel, Hingham, Mass., 1987.

[20] Mitchell, J. F. B., The "greenhouse" effect and climate change, *Rev. Geophys. Space Phys.* **27**, 115-139, 1989.

[21] North, G. R., R. F. Cahalan and J. A. Coaley, Energy balance climate models, *Rev. Geophys. Space Phys.* **19**, 91-121, 1981.

[22] North, G. R., Theory of energy-balance climate models, *J. Atmos. Sci.* **32**, 2033-2043, 1975.

[23] Oort, A. H. and E. M. Rasmusson, On the annual variation of monthly mean meridional circulation, *Monthly Weather Review*, **98**, 423-442, 1970.

[24] Oort, A. H. and E. M. Rasmusson, Atmospheric circulation statistics, NOAA Prof. Pap. No. 5, Govt. Printing Office, Washington, D.C., 323 pp, 1971.

[25] Oort, A. H., Global atmospheric circulation statistics, 1958-1973. NOAA Prof. Pap. No. 14, Govt. Printing Office, Washington, D.C., 180 pp+microfiches, 1983.

[26] Pacanowski, R., K. Dixon and A. Rosati, The G.F.D.L modulor ocean model user's guide version 1.0, GFDL Ocean Group Techn. Report #2, 1991.

[27] Rennick, M. A., The parameterization of tropospheric lapse rates in terms of surface temperature, *J. Atmos. Sci.* **34**, 854-862, 1977.

[28] Roads, J. O. and G. K. Vallis, An energy balance climate model with cloud feedbacks, *Tellus*, **36A**, 236-250, 1984.

[29] Robock, A., The seasonal cycle of snow cover, sea ice, and surface albedo, *Monthly Weather Review*, **108**, 267-285, 1980.

[30] Saltzman, B., A survey of statistical-dynamical models of the terrestrial climate, *Advances in Geophysics*, **20**, 183-304, 1978.

[31] Schneider, S. H., and T. Gal-Chen, Numeric experiments in climate stability, *J. Geophys. Res.* **78**, 6182-6194, 1973.

[32] Schneider, S. H., and C. Mass, Volcanic dust, sunspots and temperature trends, *Science*, **190**, 741-746, 1975.

[33] Sellers, W. D., A global climate model based on the energy balance of the earth-atmosphere system, *J. Appl. Meteorol.*, **8**, 392-400, 1969.

[34] Spelman, M. J. and S. Manabe, Influence of oceanic heat transport upon the sensitivity of a model climate, *J. Geophys. Res.* **89**, 571-586, 1984.

[35] Stephens, G. L., G. G. Campbell, and T. H. Vonder Haar, Earth radiation budgets, *J. Geophys. Res.* **86**, 9739-9760, 1981.

[36] Stocker T. F., D. G. Wright, and L. A. Mysak, A zonally averaged, coupled ocean-atmosphere model for paleoclimate studies, *J. of Climate* **5**, 773-797, 1992.

[37] Taljaard, J., H. van Loon, H. L. Crutcher, and R. L. Jenne, Climate of the Upper Air: Southern Hemisphere, Vol. 1, Temperatures, Dewpoints, and Heights at Selected Pressure Levels. NAVAIR 50-1c-55, Chief Naval Operations, Washington D.C., 135 pp, 1969.

[38] Van Den Dool, H. M., On the role of cloud amount in an energy balance model of the earth's climate, *J. Atmos. Sci.* **37**, 939-946, 1980.

[39] Wang, W.-C., G. Molnar, T. P. Mitchell, and P. Stone, Effects of dynamical heat fluxes on model climate sensitivity, *J. Geophys. Res.* **89**, 4699-4711, 1984.

[40] Wang, W.-C., G. Molnar, M. K. W. Ko, S. Goldenberg, and N. D. Sze, Atmospheric trace gases and global climate: a seasonal model study, *Tellus*, **42B**, 149-161, 1990.

[41] Warren, S. G. and S. H. Schneider, Seasonal simulations as a test for uncertainties in the parameterizations of a Budyko-Sellers zonal climate model, *J. Atmos. Sci.* **36**, 1377-1391, 1979.

[42] Washington, W. M. and G. A. Meehl, General circulation model experiments on the climatic effects due to a doubling and quadrupling of carbon dioxide concentration, *J. Geophys. Res.* **88**, 6600-6610, 1983.

[43] Washington, W. M. and G. A. Meehl, A seasonal cycle experiment on the climatic sensitivity due to a doubling of CO_2 with an atmospheric general circulation model coupled to a simple mixed layer ocean model, *J. Geophys. Res.* **89**, 9475-9503, 1984.

[44] Weaver, A. J., J. Marotzke, P. F. Cummins, and E. S. Sarachik, Stability and variability of the thermohaline circulation, *J. Phys. Oceanogr.* **23**, 39-60, 1993.

[45] White, R. M. and B. Saltzman, On conversions between potential and kinetic energy in the atmosphere, *Tellus*, **8**, 357-363, 1956.

[46] Zhang, S., R. G. Greatbatch and C¿ A. Lin, A reexamination of the polar halocline catastrophe and implications for coupled ocean-atmosphere modeling, *J. Phys. Oceanogr.* **23**, 287-299, 1993

Acknowledgements

We wish to thank Prof. Dr. D. Olbers for his support of this work.